Mesenchymal Stromal Cells Immunosuppress Osteoarthritis Synovial Fluid Tolerized Monocytes via IL-6

Condensed Title – MSC Modulates OA Synovial Fluid Tolerized Monocytes

Mozhgan Rasti[1,2], Aida Feiz Barazandeh[1,2], Kevin P. Robb[1,2,3], Rachel Low [1,2], Rajiv Gandhi[1,4], Sowmya Viswanathan*[1,2,3,5]

[1]Schroeder Arthritis Institute, University Health Network, Toronto, Ontario, M5T 0S8, Canada
[2]Krembil Research Institute, University Health Network, Toronto, Ontario, M5T 0S8, Canada
[3]Institute of Biomedical Engineering, University of Toronto; Toronto, Ontario, M5S 3G9, Canada

[4]Department of Surgery, Division of Orthopedic Surgery, University of Toronto, Toronto, Ontario, M5T 1P5, Canada
[5]Department of Medicine, University of Toronto, Toronto, Ontario, M5S 3H2, Canada

***Correspondence:**
Sowmya Viswanathan, PhD
Email: sowmya.viswanathan@uhn.ca

Abstract

The mechanism of mesenchymal stromal cell (MSC) interactions with monocytes/macrophages (MΦs) in knee osteoarthritis (KOA) is not fully understood. We report that synovial fluid (SF) MΦs are tolerized. Healthy donor-derived $CD14^+$ peripheral monocytes partially mimic SF MΦs tolerization, but are also activated, immunosuppressed and functionally impaired after longer exposure to complex late-stage KOA SF matrix. Classical interleukin (IL)-6 signaling in late-OA SF immunosuppresses $CD14^+$ monocytes via signal transducer and activator of transcription (STAT3) and suppressor of cytokine signaling (S*OCS3*), while toll-like receptor (TLR)4 via nuclear factor kappa-light-chain-enhancer of activated B (NF-κB) and c-Jun Terminal Kinase (JNK) drive $CD14^+$ monocyte activation. Late-OA SF semi-tolerizes $CD14^+$ monocytes with unchanged tumor necrosis factor (TNF) and CD86 expression with lipopolysaccharide (LPS) challenge. Addition of MSC(M) soluble factors enhances immunosuppression through IL-6 signaling, and nullifies late-OA SF activation effects by decreasing p-JNK and reducing TLR-mediated NF-κB and TNF. MSC(M) immunosuppressed $CD14^+$ monocytes in late-OA SF are functionally rescued with improved phagocytosis.

Graphical Abstract

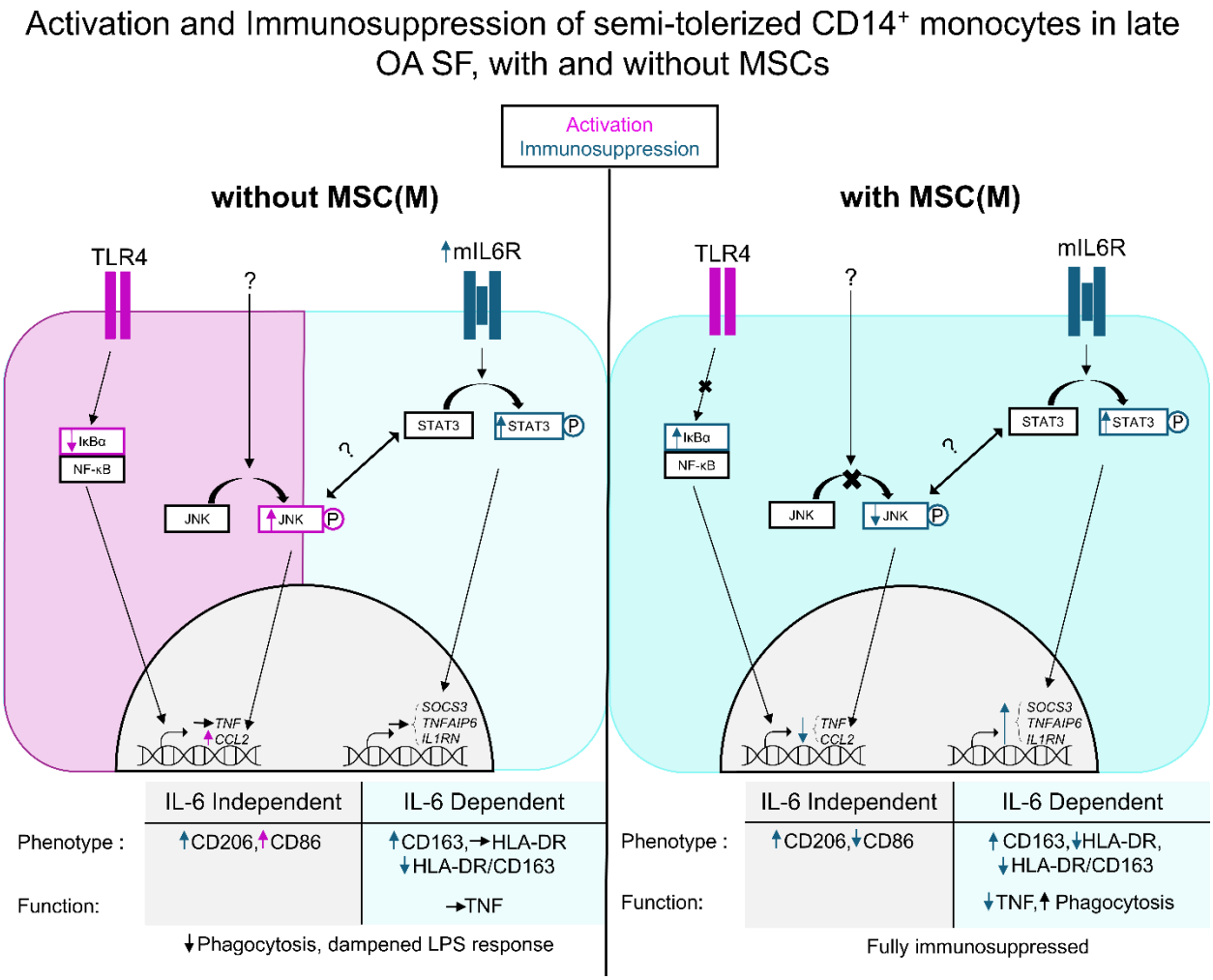

Introduction

Osteoarthritis (OA) is a chronic, low-grade inflammatory condition that affects over 15% of the global population (Steinmetz *et al.*, 2023). Infiltration and inflammation of the synovium lining membrane, or synovitis (Prieto-Potin *et al.*, 2015), contributes significantly to OA pathology (Sowers *et al.*, 2011; Zhang *et al.*, 2011). Synovitis is mediated by monocytes/macrophages (termed as MΦs), which are the most prevalent immune cells in knee OA (KOA) patients (Kraus *et al.*, 2016; Gómez-Aristizábal *et al.*, 2019); an enrichment of $CD14^{+}CD16^{+}$ intermediate synovial fluid (SF) MΦ subsets correlates with worsening patient-reported outcomes (PROMs) including knee osteoarthritis outcome scores (KOOS) in KOA patients. Mechanisms for the increase in the intermediate subset and its functional roles in KOA have not been fully investigated.

In parallel, treatment of KOA with mesenchymal stromal cells (MSC) has shown mixed clinical efficacy (Copp, Robb and Viswanathan, 2023). MSC mode of action includes reduction in inflammation and paracrine factor-mediated endogenous cartilage repair (Iijima *et al.*, 2018; Matas *et al.*, 2019; Copp, Robb and Viswanathan, 2023). Autologous bone marrow MSC(M) reduce joint-specific SF levels of intermediate $CD14^{+}CD16^{+}$ MΦs (Chahal *et al.*, 2019). Efferocytosis of intra-articularly injected isogenic murine MSC(M) changes the synovial macrophages to pro-resolving phenotypes, in an experimental model of post-traumatic OA (Hamilton *et al.*, 2019). Thus, evidence is highly supportive of MSC interactions with synovial tissue macrophages and SF MΦs, as a primary mode of action in KOA. KOA patient SF is complex and contains multiple factors, including pro-inflammatory cytokines (Smith *et al.*, 1997), chemokines (Zhang *et al.*, 2023),

complement factors (Assirelli *et al.*, 2020), extracellular matrix (ECM) fragments (Midwood *et al.*, 2009), toll-like receptor (TLR) ligands, endotoxin (Huang *et al.*, 2016) that have a licensing effect on MSC to trigger their immunomodulatory activities. MSC(M) licensed by SF from KOA patients produce high levels of chemokine (C-C motif) ligand 2 (CCL2) and IL-6 (Gómez-Aristizábal *et al.*, 2017).

IL-6 is a pleiotropic cytokine with both pro- and anti-inflammatory, cell- and disease-specific roles (Kishimoto, Kang and Tanaka, 2015). MSC-secreted IL-6 has pro-resolving effects on MΦs (Kim and Hematti, 2009). Paradoxically, elevated levels of circulating IL-6 are predictors of radiographic KOA (Livshits *et al.*, 2009) and correlate with increased pain and worsening function in KOA (Ahmed, Soliman and Elwan, 2023). Given that MSC result in analgesic and function-preserving effects (Copp, Robb and Viswanathan, 2023), MSC-secreted factors, including IL-6 are hypothesized to play a regulatory role in the context of KOA.

In this study, we first report that SF MΦs are tolerized based on in vitro LPS re-challenge. Long term exposure of $CD14^+$ peripheral monocytes from healthy donors to late-OA SF similarly induces semi-tolerization. Additionally, the complex late-OA SF matrix also activates, immunosuppresses and functionally impairs $CD14^+$ peripheral monocytes. Using phenotypic markers, signaling kinases and functional readouts, we elucidate roles for canonical IL-6 signaling in late-OA SF in immunosuppressing $CD14^+$ peripheral monocytes, and identify roles for TLR (4) mediated NF-κB pathway and other factors in the late-OA SF via JNK pathways that contribute to $CD14^+$ peripheral monocyte activation. Despite this, the $CD14^+$ monocytes exposed to late-OA SF are semi-tolerized and

functionally impaired; they do not produce additional TNF, even with LPS challenge, and have reduced phagocytic capacity. Addition of MSC(M) enhances the IL-6 mediated immunosuppressive effects and negates the late-OA SF activation effects. Importantly, the MSC(M) educated $CD14^+$ monocytes have reduced TNF and improved phagocytosis functionality.

Results

Late-Stage OA SF has pro-inflammatory mediators and MΦs with a mixed phenotypic profile

SF from mid-stage (defined as Kellgren Lawrence (KL) Grade II-early Grade III) and late-stage (defined as KL Grade late III-IV; Table S1) KOA patients were measured for various cytokines, chemokines, and alarmins (Table S2). All factors were specifically increased in late-stage OA patients, as demonstrated by an area under the ROC curve of ≥ 0.74 (Fig. S1A-D). IL-6 and CCL2 increased in late-OA SF vs. non-OA SF (Fig. 1A,B). IL-6 showed a non-significant increase in mid-OA SF due to data variability, but CCL2 demonstrated a substantial augmentation compared to non-OA SF (Fig. 1A,B). S100A8/9 and IL-8 significantly increased from mid-to late-stage OA SF (Fig. 1C,D).

MΦs from late-OA SF were immunophenotyped with classical $CD14^+CD16^{neg}$ and double-positive, intermediate $CD14^+CD16^+$ MΦs subsets being the most abundant, as before (Gómez-Aristizábal *et al.*, 2019) (Fig. 1E). Classical, intermediate and non-classical $CD14^{lo}CD16^+$ SF MΦs all expressed CD163, CD206 and Human Leukocyte Antigen-DR isotype (HLA-DR), albeit at varying ratios (Fig. 1F-H). While the expression of CD163, CD206 and HLA-DR all increased within the intermediate MΦs, the balance

was tipped towards a reduced HLA-DR/CD163 mean fluorescence intensity (MFI) expression ratio (Fig. 1I), indicative of a tolerized, intermediate SF MΦ subset. There were no significant differences in CD163 and HLA-DR MFI expressions between classical and non-classical MΦ subsets, although the classical but not non-classical MΦ subset had increased HLA-DR/CD163 expression ratios (Fig. 1, F,H,I).

Challenge with lipopolysaccharide (LPS) for 4h with or without additional 48h tolerization with LPS showed no significant changes in CD86, HLA-DR, CD163, CD206 or intracellular IL-1 and TNF MFI expression. This data is suggestive of in vivo tolerization of SF MΦs by late-OA SF, as cells were not further tolerized or challenged in vitro (Fig. 1J).

CD14^{+} peripheral monocytes exposed to OA SF serve as a surrogate for OA SF MΦs

To perform more detailed analyses on intermediate SF MΦs, which are the main effector MΦ subsets in late-stage OA joints correlating with worsening patient-reported outcome measures (Gómez-Aristizábal *et al.*, 2019), we require 5 × 10^{6} MΦs/run. We routinely isolate 3-10 ×10^{4} SF MΦs, insufficient for multivariate analyses without further cell culturing and culture induced modifications. To circumvent this limited supply, peripheral blood human CD14^{+} monocytes were isolated and exposed to mid- or late-OA SF for 3 days in culture. This resulted in increased frequency of intermediate CD14^{+}CD16^{+} monocytes and a concomitant decrease in classical CD14^{+}CD16^{neg} monocytes (Fig. 2A; S2A), mimicking the frequency changes of MΦs in OA SF (Gómez-Aristizábal *et al.*, 2019).

We noted partial tolerization effects of longer term (72h) exposure to late-OA SF based on unchanged TNF production after LPS-challenge, compared to LPS-stimulated $CD14^+$ monocyte controls (without late-OA SF exposure, Fig. 2J). CD163, CD206 MFI were unchanged by LPS challenge after late-OA SF exposure. However, HLA-DR MFI was increased, not decreased, and CD86 was unchanged by LPS challenge after late-OA SF exposure, indicative of partial tolerization in healthy donor $CD14^+$ monocytes. Peripheral $CD14^+$ monocytes from late-OA patients, on the other hand, had unchanged HLA-DR and CD86 by LPS challenge after late-OA SF exposure, arguing for more tolerized $CD14^+$ monocytes from OA patients vs. healthy donors (Fig. 2C). Both $CD14^+$ monocytes from healthy vs. OA donors, however showed unchanged HLA-DR/CD163 ratios with LPS challenge after late-OA SF exposure, arguing for overall similar tolerization profiles (Fig. 2D). Given their largely overlapping profiles, we used readily available $CD14^+$ monocytes from healthy (vs. OA patient) donors, exposed to OA SF for the remainder of the study.

The observed increase in the percentages of $CD14^+CD16^+$ monocytes by exposure to both mid- or late-OA SF was abrogated by an IL-6 neutralizing antibody (Nordan and Potter, 1986) (Fig. 2B; S2B), suggestive of endogenous IL-6 stimulation within OA SF. $CD14^+$ monocytes treated with supraphysiological levels of recombinant IL-6 as a positive control showed increased CD163, CD206 MFI (Fig. 2E,F) and decreased HLA-DR/CD163 MFI ratio (Fig. 2I) without effects on HLA-DR or CD86 MFI (Fig. 2G,H). There were no dose-dependent effects at various IL-6 concentrations tested (Fig. S2C).

The addition of late-OA SF to $CD14^+$ monocytes partially mimicked the effects of supraphysiological IL-6 on CD163, CD206 MFI (Fig. 2E,F) and the HLA-DR/CD163 MFI ratio (Fig. 2I). However, late-OA SF, unlike supraphysiological IL-6 significantly increased

CD86 expression, relative to untreated CD14$^+$ monocytes from healthy but not OA patient donors (Fig. 2C,H). Addition of neutralizing IL-6 antibody nullified late-OA SF effects on CD163 and HLA-DR/CD163 MFI ratio (Fig. 2E,I) but not CD206, HLA-DR or CD86 MFI (Fig. 2F-H), suggestive of IL-6-dependent and independent effects. Addition of mid-OA SF to CD14$^+$ monocytes had similar trends but was not significant (Fig. 2E-I).

To explore other factors in late-OA SF contributing to the observed phenotypic effects, 1µg/mL (physiological levels, Fig. 1C) of S100A8/9, an endogenous TLR ligand, was added. CD163, CD206 and CD86 MFI were reduced with S100A8/9, compared to late-OA SF stimulation, with a concomitant increase in HLADR/CD163 MFI ratio (Fig. S2D-H). Physiological levels of S100A8/9, therefore, did not replicate the effects of late-OA SF on CD14$^+$ monocyte phenotypic changes. Addition of a TLR inhibitor, TAK242 (Ii *et al.*, 2006), to late-OA SF also did not abrogate any phenotypic effects of endogenous S100A8/9 in late-OA SF (Fig. S2D-H).

To test the functional effects of late-OA SF, TNF soluble factor production by CD14$^+$ monocytes after a short-LPS challenge was measured and showed increases (Fig. 2J). Addition of late-OA SF (with LPS re-challenge), however did not change TNF levels, confirming partial tolerization effects of late-OA SF on peripheral CD14$^+$ monocytes from healthy donors. Supraphysiological levels of IL-6 significantly reduced TNF production; neutralizing IL-6 antibody with late-OA SF conversely, significantly increased TNF secretion, confirming an endogenous IL-6 mediated effect (Fig. 2J). S100A8/9, while not mimicking late-OA SF in modulating CD14$^+$ monocyte phenotypically, did replicate late-OA SF in terms of unchanged TNF production; addition of TAK242 to late-OA SF also significantly suppressed TNF production (Fig. S2I). We thus identify a role for TLR4

pathway in TNF production by CD14$^+$ monocytes in late-OA SF. TNF production in mid-OA SF was significantly lower than late-OA SF (Fig. 2J), further confirming reduced pro-inflammatory mediators in mid- vs. late-OA SF (Fig. 1A-D).

IL-6 signaling in OA SF is mediated through canonical, not trans-signaling

IL-6 canonical signaling occurs through membrane IL-6 receptor (mIL-6R) while trans-signaling occurs through soluble IL-6 receptor (sIL-6R) and gp130 (Fig. 3A). IL-6 increased from mid- to late-stage OA (Fig. 1A) but sIL-6R levels decreased (Fig. 3B), arguing against IL-6 trans-signaling. To clarify whether IL-6 signaling to CD14$^+$ monocytes in late-OA SF was canonical- or trans-signaling, we added physiological levels of IL-6 (0.5 ng/mL) with or without physiological sIL-6R (10 ng/mL); there were no significant changes in CD163, CD206, HLA-DR or CD86 MFI expression on CD14$^+$ monocytes, supportive of the absence of competitive trans-signaling (Fig. 3C-F). This was replicated by the treatment of CD14$^+$ monocytes with soluble gp130 (sgp130, 10ng/mL) in the presence of late-OA SF (Fig. 3C-F). Additionally, mIL-6R expression increased on CD14$^+$ monocytes exposed to mid- or late-OA SF (Fig. 3G), confirming the dominance of classical IL-6 signaling. Further, there was a complete absence of detectable levels of the IL-6-sIL-6R complexes in both mid- and late-OA SF (undetectable in 91 of 96 samples), readily found in inflammatory arthritic controls (Fig. 3H).

OA SF differentially activates signaling pathways in CD14$^+$ monocytes depending on the duration of IL-6 exposure

We noted extensive activation of MAPK and STAT kinases in CD14$^+$ monocytes treated with late-OA SF using a human phospho-kinase array (Fig. S3A). Although multiple MAP kinases were evaluated, only significant changes in the phosphorylation (p) levels of c-

Jun Terminal Kinase (JNK) were observed (Fig. S3B-D). Normalized p-JNK levels increased after 10 min of exposure to late-OA SF, while normalized p-STAT3 increased significantly after 1h of exposure; both remained elevated for 72h (Fig. S3D,E).

To explore the role of IL-6 and S100A8/9 signaling in late-OA SF, $CD14^+$ monocytes were pre-treated with neutralizing IL-6 antibody or TLR inhibitor, TAK242 and exposed to late-OA SF for short- or long exposure times (Fig. 4A). Controls included treatment with IL-6 or S100A8/9 for short (40 min, timing based on Fig. S3F) and longer exposure times (24h; Fig. 4A). Short-(Fig. 4B,D) and longer (Fig. 4C,D) exposures to IL-6 significantly but differentially increased normalized p-STAT3 levels, relative to non-stimulated controls. Late-OA SF short and long exposure also increased normalized p-STAT3 relative to non-stimulated controls (Fig. 4B-D), although only longer-exposure times mimicked supraphysiological IL-6 (Fig. 4C,D). Conversely, S100A8/9 reduced normalized p-STAT3 at both longer and short exposures, relative to late-OA SF (Fig. 4B-D; S3F), confirming that S100A8/9 does not fully re-capitulate late-OA SF effects. Pre-treatment of $CD14^+$ monocytes with IL-6 antibody also reduced normalized p-STAT3 at both long and short exposures, relative to late-OA SF stimulation (Fig. 4B,D). TAK242, on the other hand, significantly elevated normalized p-STAT3 levels at short but not longer exposures (Fig. 4B-D). TAK242 inhibition thus replicates differential IL-6 short vs. long-term effects and overrides S100A8/9 mediated inhibition of STAT3 phosphorylation (Fig. 4B-D; S3F). Together, these data support IL-6 and TAK242-inhibitor-mediated increases in STAT3 phosphorylation, especially in the short term; these effects were blunted at longer exposures, suggesting the presence of feedback mechanisms.

By contrast, both IL-6 and S100A8/9 stimulation did not significantly alter normalized p-JNK levels at either short or longer exposures in $CD14^+$ monocytes, implicating other factors in late-OA SF for observed p-JNK activation (Fig. 4B,C,E). Although IL-6 did not impact JNK phosphorylation, pre-treatment with IL-6 neutralizing antibody, in the presence of late-OA SF, significantly decreased normalized p-JNK at short exposures. Long-term exposure to late-OA SF and IL-6 neutralizing antibody restored p-JNK levels to short-exposure levels of late-OA SF. This implies longer-term late-OA SF tolerization effects on p-JNK that are not susceptible to IL-6 modulation. Conversely, TAK242 inhibition in late-OA SF increased normalized p-JNK levels at short but not long exposure times; long TAK242 exposures mimicked late-OA SF tolerization (Fig. 4B,C,E). Other JNK inhibitors, including SP600125 also did not inhibit JNK phosphorylation even at longer exposure times; the effects of late-OA SF seem to override the effects of these inhibitors albeit with increased STAT3 phosphorylation, suggesting complex, temporally regulated inhibitory interplay between STAT3 and JNK phosphorylation (Fig. S3G).

IL-6 increased normalized, total protein levels of nuclear factor of kappa light polypeptide gene enhancer in B-cells inhibitor alpha (IκBα) at short and longer exposures relative to late-OA SF stimulations; the effects of endogenous IL-6 in late-OA SF were reversed by addition of IL-6 neutralizing antibody (Fig. 4B,C,F). S100A8/9, on the other hand, mimicked late-OA SF exposure, especially at shorter vs. longer exposures, reducing normalized IκBα levels, both of which were abrogated by TAK242 (Fig. 4B,C,F). Canonically, IκBα inhibits bound NF-κB; it's degraded in the cytosol and releases NF-κB for further downstream signaling (Yan *et al.*, 2020).

Differential kinetics of IL-6-mediated short vs. long exposures indicated activation of feedback inhibitors, such as suppressor of cytokine signaling 3 (*SOCS3*), a known modulator of IL-6 signaling (Wang *et al.*, 2003). As expected, *SOCS3* increased after longer IL-6 exposure (Fig. 4G). Surprisingly, SOCS3 and p-STAT3 both increased with long-term late OA SF exposure, relative to non-treated $CD14^+$ monocyte controls (Fig. 4D,G). Adding IL-6 neutralizing antibody to late-OA SF, dually reduced IL-6 induced SOCS3 and p-STAT3 (Fig. 4D,G). Longer-term exposure to S100A8/9 similarly reduced both SOCS3 and p-STAT3 (Fig. 4D,G); shorter S100A8/9 exposure also attenuated STAT3 phosphorylation even in the presence of supraphysiological levels of IL-6 and late-OA SF (Fig. S3F). As expected, TAK242 inhibition reversed the effect of endogenous S100A8/9 in late-OA SF given known S100A8/9 binding to TLR4 (Vogl et al., 2007; Fig. 4B,D, G; S3F). Thus, differential STAT3 phosphorylation by various treatments of $CD14^+$ monocytes in late-OA SF is not fully explained by *SOCS3* upregulation and indicates other contributing downstream effectors.

CCL2, downstream of both JNK and IL-6 signaling (Li et al., 2011), may be one such effector. *CCL2* was increased by long-term exposure to late-OA SF and TAK242 inhibition and decreased by IL-6 neutralizing antibody, relative to untreated $CD14^+$ monocytes (Fig. 4H). Changes to *CCL2* correlated with JNK phosphorylation mediated by short late-OA SF exposures, with or without IL-6 neutralizing antibody or TAK242 inhibition (Fig. 4E, H). However, there was no correlation between *CCL2* and JNK phosphorylation with longer exposures to late-OA SF (Fig. 4E, H), indicative of other pathways in mediating *CCL2*.

TNF, downstream of JNK and NF-κB activation (Han *et al.*, 2012; Delprat *et al.*, 2020) was unchanged by late-OA SF stimulation; however, it was inversely correlated with the

opposing effects of IL-6 and S100A8/9 on IκBα activation (Fig. 4F,I). IL-6 neutralizing antibody increased *TNF*, correlating with reduced IκBα activation relative to late-OA SF alone; TAK242 decreased *TNF*, correlating with increased IκBα activation (Fig. 4F,I).

Together, longer-term late-OA SF exposure activates STAT3 and JNK phosphorylation and reduces IκBα levels in $CD14^+$ monocytes; downstream effectors included, elevated *CCL2 and* unchanged *SOCS3* and TNF. These and other downstream effectors modulate the long-term effects of late-OA SF on kinase activation and result in a net semi-tolerized profile of $CD14^+$ monocytes.

MSC(M) countered late-OA SF effects on $CD14^+$ monocytes via IL-6 dependent and independent pathways

$CD14^+$ monocytes co-cultured directly with MSC(M) alone show increased CD163, CD206 MFI, reduced HLA-DR MFI, and HLA-DR/CD163 MFI ratio (Fig. 5A-F; S4A-E). MSC(M) maintained the tolerized $CD14^+$ monocyte phenotype in late-OA SF, and in fact further reduced HLA-DR, CD86 MFI and HLADR/CD163 MFI ratios, speaking to additional immunosuppressive effects. In fact, addition of MSC(M) to late-OA SF synergistically and significantly increased CD163 and CD206 MFI (Fig. 5B,C). IL-6 neutralizing antibody reversed MSC(M) mediated effects on CD163, HLA-DR MFI but not on CD206 or CD86 MFI or HLA-DR/CD163 MFI ratio (Fig. 5B-F). Adding S100A8/9 to MSC(M) direct co-cultures with $CD14^+$ monocytes did not alter the higher MFI expression of CD163, CD206 or increase HLA-DR MFI or HLA-DR/CD163 MFI ratio (Fig. S4A-E).

We further re-challenged $CD14^+$ monocytes from healthy and late-OA donors with LPS, with and without late-OA SF or MSC(M), to identify any tolerizing effects of MSC(M). MSC(M) further reduced HLA-DR and CD86 MFI in LPS-stimulated conditions, both with

and without late-OA SF exposure (Fig. S4F); HLA-DR/CD163 MFI ratio was also reduced by MSC(M), relative to LPS re-challenged $CD14^+$ monocytes (Fig. S4G). However, $CD14^+$ monocytes from healthy and OA donors were comparable in late-OA SF with LPS challenge, both in the presence and absence of MSC(M). Together, this data confirmed semi-tolerization of $CD14^+$ monocytes by late-OA SF exposure and further immunosuppression, but not tolerization by addition of MSC(M).

18-21% of MSC(M) in late-OA SF demonstrated early apoptosis, a significant increase compared to MSC(M) in normal medium at 24h, but not at 48 or 72h; this was a donor-dependent effect with one of three MSC(M) donors showing greater susceptibility (Fig. S5A). IL-6 neutralizing antibody rescued the late-OA SF apoptosis; S100A8/9 did not potentiate MSC apoptosis arguing for other factors in late-OA SF, responsible for this effect.

Next, we tested soluble factor effects of MSC(M). Secondary $CD14^+$ monocytes were treated with conditioned medium (CM) from primary direct co-cultures of $CD14^+$ monocytes with MSC(M), licensed by late-OA SF (Fig. 6A). Normalized p-STAT3 and IκBα levels increased significantly, while normalized p-JNK was reduced significantly, relative to late-OA SF alone, despite the long-term exposure (Fig. 6B-E). Pre-treatment with IL-6 neutralizing antibody nullified some of the licensed MSC(M) CM effects, reducing p-STAT3 and increasing p-JNK (Fig. 6B-D); there was no effect on normalized IκBα (Fig. 6B,E). Together, licensed MSC(M) CM increased p-STAT3 and reduced p-JNK in an IL-6-dependent manner while increasing IκBα in an IL-6-independent manner, speaking to its net anti-inflammatory effect.

Downstream effectors, including *SOCS3,* were significantly upregulated by late-OA SF licensed MSC(M) CM (Fig. 6F), mimicking the effects of supraphysiological IL-6 (Fig. 4G). Pre-treatment with IL-6 neutralizing antibody nullified this increase, confirming IL-6-mediated MSC(M) soluble effects (Fig. 6F). Licensed MSC(M) CM also increased IL-6 downstream genes, including TNF-alpha Induced Protein 6 (*TNFAIP6*) and IL-1 Receptor Antagonist (*IL-1RN*) (Fig. S5B,C). *CCL2* and *TNF* were both suppressed by late-OA-SF licensed MSC(M) in $CD14^+$ monocytes; *TNF,* but not *CCL2* was suppressed in an IL-6-dependent manner in late-OA SF licensed MSC(M) CM (Fig. 6G,H). Late OA-SF licensed MSC(M) CM also increased prostaglandin-endoperoxide synthase 2 (*PTGS2*) in an IL-6 independent manner (Fig. S5D).

In secondary $CD14^+$ monocytes cultured with CM from late-OA SF licensed MSCs, TNF soluble factor induced by long-term exposure to late-OA SF and LPS stimulation was significantly attenuated by licensed MSC(M) CM addition, even with LPS re-challenge (Fig. 6I). This rescue effect was abrogated by pre-treatment with IL-6 neutralizing antibody (Fig. 6I). The $CD14^+$ monocytes morphology in late-OA SF licensed MSC(M) CM were larger, more spindle-shaped and took on a macrophage appearance (Fig. S5E). Late-OA licensed MSC(M) CM also rescued phagocytotic activity, which was reduced by late-OA SF exposure, in an IL-6 dependent manner (Fig. 6F).

Discussion

We evaluated mechanisms of MSC(M) mediated immunosuppression and reduced activation of $CD14^+$ peripheral monocytes in late-OA SF to understand clinically reported MSC(M) analgesic and functional improvement effects in KOA patients (Chahal *et al.*, 2019; Copp, Robb and Viswanathan, 2023). We had previously shown that MSC(M)

reduce the frequency of $CD14^+CD16^+$ intermediate SF MΦs in KOA patients (Chahal *et al.*, 2019); $CD14^+CD16^+$ intermediate MΦs are the dominant MΦ subset in late-OA SF, and their frequency correlates inversely with PROMS using the Knee Osteoarthritis and Outcome Scores (KOOS) indices (Gómez-Aristizábal *et al.*, 2019). We used $CD14^+$ peripheral monocytes exposed to complex mixture of activating, suppressing and tolerizing factors in late-OA SF in the presence and absence of MSC(M) to understand the basal profile of monocytes in OA SF, and the rescue effects of MSC(M).

$CD14^+$ peripheral monocytes exposed to late-OA SF had increased frequency of intermediate $CD14^+CD16^+$ monocytes, concordant with the activated status of monocytes, exposed to inflammatory disease stimuli (Rogacev *et al.*, 2012; Metcalf *et al.*, 2017; Yin *et al.*, 2022). This shift to intermediate monocytes was IL-6 mediated as this effect was mitigated by blocking IL-6 in late-OA SF.

$CD14^+$ monocytes exposed to late OA SF were semi-tolerized, similar to monocytes in patients with active sepsis (Shalova *et al.*, 2015); this was based on unchanged CD86 (Gu *et al.*, 2022) and TNF production, but increased HLA-DR expression (Fumeaux and Pugin, 2002) by LPS re-challenge in vitro. They thus partially mimic endogenous SF MΦs, which exhibit a tolerized profile with unchanged phenotypic markers, IL-1 and TNF even with LPS challenge, consistent with other reports (Mikulkova *et al.*, 2024).

However, $CD14^+$ monocytes are only partially tolerized. This is because the late-OA SF contains numerous factors including IL-6, S100A8/9 alarmins, endotoxins (Huang *et al.*, 2016), pro-inflammatory cytokines (Mathiessen and Conaghan, 2017), complement activators (Gobezie *et al.*, 2007), ECM fragments (Midwood *et al.*, 2009). Late-OA SF

also contains elevated but variable levels of pro-inflammatory cytokines (Kraus *et al.*, 2016) and low levels of other pro-inflammatory mediators like IL-15 and TNF (Özler *et al.*, 2016; Gómez-Aristizábal *et al.*, 2017). Late-OA SF thus does not induce a fully pro-inflammatory, fully tolerized, or fully immunosuppressive phenotype in $CD14^+$ peripheral monocytes; rather there is a mixed profile, speaking to the presence of multiple factors in dynamic, fluctuating ratios.

MSC(M) addition to late-OA SF enhances immunosuppression of peripheral $CD14^+$ monocytes. Given previous observations that MSC(M), licensed by factors present in OA SF increased secretion of IL-6 (Gómez-Aristizábal, Kim and Viswanathan, 2016), we explored the immunosuppressive effects of IL-6 on $CD14^+$ monocytes. IL-6 has paradoxical roles in OA; increased levels of IL-6 correlate with increased OA severity (Li *et al.*, 2020; Ahmed, Soliman and Elwan, 2023); circulating levels of IL-6 are predictive of OA incidence (Wiegertjes, Loo and Davidson, 2020). However, IL-6 knockout male mice develop more severe spontaneous OA (de Hooge *et al.*, 200), while IL-6 knockout experimental OA models show increased cartilage damage (Ryu *et al.*, 2011). There is thus context-dependent IL-6 protective or pathogenic signaling in OA.

IL-6 binds to IL-6R, dimerizes gp130 and induces classical signaling via activation of JAK/STAT pathways (Kishimoto, Akira and Taga, 1992). IL-6R is only expressed on hepatocytes and leukocytes (Hibi *et al.*, 1990; Heinrich *et al.*, 2003); classical signaling is thus restricted to these cells and produces an anti-inflammatory signal (Rose-John, 2017). IL-6 classical signaling is tightly regulated by SOCS3 (Babon, Varghese and Nicola, 2014). Signaling through sIL-6R, generated by proteolytic cleavage of mIL-6R or through transcription of alternatively spliced IL-6R mRNA (Lust et al., 1992; Riethmueller et al.,

2017) results in trans-signaling (Rose-John and Heinrich, 1994) which is broader given the ubiquitous expression of gp130 receptors on multiple cell types; trans-signaling results in stronger activation of intracellular signaling (Reeh *et al.*, 2019) and is reported to be pro-inflammatory (Rose-John, 2017).

To our knowledge, we are the first to report SF levels of sIL-6R (Wu *et al.*, 2018) in KOA patients vs. non-OA samples. sIL-6R levels were reduced with increasing OA stages; there was an absence of detectable sIL-6R-IL-6 complexes in OA SF. Our data thus strongly argue for IL-6 mediated classical signaling on SF MΦs and peripheral $CD14^+$ monocytes, which express mIL-6R (Bauer *et al.*, 1989).

Our data support IL-6 classical signaling in immunosuppressing $CD14^+$ monocytes in late-OA SF via p-STAT3 and *SOCS3*. SOCS3 mediates temporal activation of feedback inhibition of IL-6 stimulated STAT signaling (Babon, Varghese and Nicola, 2014). IL-6 neutralizing antibody with long-term late-OA SF exposure reduced *SOCS3* and p-STAT3 but increased p-JNK. Together, this may explain the mixed clinical effects of IL-6 neutralizing antibody in OA (Richette *et al.*, 2021). Our data also point to co-variance of *SOCS3* gene expression and STAT3 phosphorylation in long-term exposure to late-OA SF, contrary to previously reported inverse correlations (Yasukawa *et al.*, 2003). This may be because we measured *SOCS3* at the transcript rather than protein levels, and/or this may indicate partial tolerization effects of late-OA SF.

We next explored the role of alarmins found in late-OA SF. Addition of S100A8/9 could only partially recapitulate late-OA SF effects. S100A8/9 did not replicate increases in JNK phosphorylation seen with late-OA SF exposure. Adding TAK242, a TLR4 inhibitor and

other JNK inhibitors increased short-term but not long-term JNK phosphorylation in late-OA SF. S100A8/9, however replicated late-OA SF in decreasing IκBα levels, without changes to TNF protein and gene levels, aligned with partial activation and tolerization mediated by late-OA SF. TAK242 inhibitor with late-OA SF exposure reversed these effects, but increased *CCL2,* which ma*y* be explained by alternate pathway activation including phosphatidylinositol 3-kinase (PI-3K)/Akt (Chen *et al.*, 2019). Thus, we postulate the involvement of canonical TLR4 signaling (Wei *et al.*, 2024) in late-OA SF through NF-κB but not JNK pathways.

We also observed an interplay between TLR-mediated short-term effects on JNK and STAT3 pathways and long-term effects mediated by IL-6 signaling on STAT3 and JNK phosphorylation. This is consistent with previous reports of elevated phosphorylated STAT3 in bone marrow-derived macrophages in S100A8/9 double knock-out mice (Russo *et al.*, 2022).

$CD14^+$ monocytes exposed directly to MSC(M) in late-OA SF had enhanced immunosuppression and reduced activation as indicated by increased CD206, CD163 MFI, p-STAT3, IκBα, *SOCS3* levels, and reduced HLA-DR, CD86, p-JNK, *CCL2*, TNF protein and gene levels. $CD14^+$ monocytes in direct coculture with MSC(M) in mid-OA SF had a similar phenotypic profile as in late-OA SF, but without significant reductions in HLA-DR; this may again speak to the altered ratios of various mediators in mid- vs. late-OA SF.

IL-6 classical signaling from late-OA SF licensed MSC(M) CM dually increased p-STAT3 and *SOCS3,* thereby attenuating the mixed effects of late-OA SF, and partially explaining

MSC(M) beneficial effects. Long-term exposure to late-OA SF did not change *SOCS3,* but increased p-STAT3. Our findings mirror observations that human umbilical cord blood-derived MSC mitigated LPS-induced pro-inflammatory polarization of alveolar macrophages in a SOCS-dependent manner (Kim *et al.*, 2023); blocking SOCS abolished MSC rescue effects, including attenuations in frequency of $CD86^+$ macrophages and TNF levels.

Soluble factors in late OA-SF licensed MSC(M) CM also acted through the JNK/STAT3 axis by reducing JNK phosphorylation, increasing STAT3 phosphorylation and IκBα level in secondary $CD14^+$ monocytes.

Given that between 18-21% of MSC(M) were undergoing early apoptosis within 24 hours of exposure to late-OA SF, we cannot rule out efferocytosis of MSC(M) by $CD14^+$ monocytes under direct culture conditions as reported in other disease models (Galleu *et al.*, 2017; Lv *et al.*, 2020) and in experimental OA model (Hamilton *et al.*, 2019). However, late-OA SF licensed MSC(M) CM was used to investigate signaling kinase activity, gene expression downstream of signaling kinases, functional phagocytosis and TNF production by secondary $CD14^+$ monocytes, speaking to the effects of MSC(M) soluble factors. These soluble factors may still be mediated by extracellular vesicles and/or apoptotic bodies produced by apoptotic MSC(M) (in addition to non-apoptotic MSC(M).

Soluble factors in late-OA SF licensed MSC(M) CM increased *TNFAIP6 e*ncoding for TNF-stimulated gene 6 protein (TSG-6); *PTSG2,* which encodes cyclooxygenase (Bouffi *et al.*, 2010) and I*L-1RN* in $CD14^+$ monocytes. TSG-6, an important MSC

immunoregulator (Prockop, 2016), inhibits JNK and NF-κB activation (Mittal *et al.*, 2016; Zhang *et al.*, 2017) and promotes transition to anti-inflammatory macrophages (Mittal *et al.*, 2016; Zhang *et al.*, 2017). Cylcooxygenase, also known as *PTSG2* gene (Bouffi *et al.*, 2010) converts arachidonic acid to prostaglandin (PG). Although PG is associated with OA pathology (Amin *et al.*, 1997; Li *et al.*, 2009), dual roles for PG have been reported including attenuation of inflammatory genes (Maekawa *et al.*, 2021). Increased IL-1R antagonist has demonstrated protective effects in animal models of OA (Evans, 2018) but not in clinical trials (Yu *et al.*, 2023).

$CD14^+$ monocytes took on a differentiated macrophage morphology in the presence of late-OA SF, and even more so with late-OA licensed MSC(M) CM. IL-6 promotes macrophage differentiation by enhancing macrophage colony-stimulating factor (M-CSF) receptor expression, enabling autocrine M-CSF signaling (Chomarat *et al.*, 2000). However, semi-tolerized $CD14^+$ monocytes with late-OA SF exposure have impaired functionality as measured by phagocytosis, congruent with disrupted efferocytotic function of peripherally derived macrophages in OA patients with higher disease activity (Del Sordo *et al.*, 2023). Licensed MSC(M) CM rescued this phagocytotic capacity.

This study has a few limitations. We could not directly assess SF MΦs with multivariate analysis, as the quantity of MΦs from SF is limited. We used peripheral $CD14^+$ monocytes treated with OA SF to mimic SF MΦs. However, $CD14^+$ peripheral monocytes exposed to late-stage OA SF exhibited a partially tolerized profile, even with LPS challenge. Although SF MΦs were more tolerized than $CD14^+$ peripheral monocytes exposed to late-OA SF, studying $CD14^+$ peripheral monocytes in isolation is useful to monitor cellular changes and mechanisms; this is difficult to do in situ with multiple joint cell types inducing

confounding effects. Others have similarly used peripheral monocytes, tolerized with LPS and shown overlapping, but also important transcriptomic divergences with synovium tissue macrophages (C. Wang *et al.*, 2024).

Another limitation is that we sourced peripheral $CD14^+$ monocytes from healthy individuals which did not fully mimic the tolerized profile of peripheral $CD14^+$ monocytes from OA patients. This is likely due to systemic effects of OA. Nonetheless, $CD14^+$ monocytes from healthy and OA donors showed similar HLA-DR/CD163 profiles with late-OA SF exposure and LPS challenge and similar responses to MSC(M) boosting confidence in the extendibility of results from healthy to OA $CD14^+$ monocytes.

MSC(M) immunosuppressed and nullified activation of peripheral $CD14^+$ monocytes exposed to late-OA SF. Although MSC(M) mimicked IL-6 classical signaling, and mitigated some S100A8/9 effects, it neither fully reproduced the extent of MSC(M) immunosuppressive effects. This is highly suggestive of other MSC soluble factors, including *PTSG2*, *TNFAIP6*, and *IL-1RN*, which are elevated in CD14+ monocytes by late-OA SF-licensed MSC (M) CM and may ultimately be responsible for the observed immune suppression.

Taken together, MSC(M) through IL-6 classical signaling, further immunosuppressed, partially tolerized peripheral $CD14^+$ monocytes in late-OA SF. MSC(M) also modulated $CD14^+$ monocytes with late-OA SF in an IL-6 independent manner, likely by modulating TLR4 signaling. MSC(M) promoted $CD14^+$ macrophage differentiation and rescued phagocytotic functionality. Our data thus provides IL-6-dependent and independent mechanisms of soluble factors in licensed MSC(M) CM that generate an immune-

suppressed, CD14^{+} monocyte profile in late-OA SF, reminiscent of absolutely tolerized macrophages (Huber *et al.*, 2017).

Materials and methods

SF sample collection

SF samples were either collected from patients diagnosed with KOA (n=139, REB 14-7483) or from non-OA screened cadaveric donors (n=11, REB 24-566). Cadaveric samples were provided by collaborator, R Krawetz. Patients with KOA had up to 5 mL of SF aspirated at the time of clinical intervention (prior to intra-articular injection, arthroscopy, or arthroplasty). KOA patients met the American College of Rheumatology criteria for symptomatic KOA (Roos *et al.*, 1998). Radiographs from patients were used for KL grading. Demographic information on patients and their KL grading is in Table S1. Psoriatic arthritis (n=2) and rheumatoid arthritis SF sample (n=1) were collected under REB 21-5591 and REB14-7483, respectively.

SF MΦs immunophenotyping

Collected SF samples were stored at 4 °C and processed within 24 hours of acquisition. Samples exhibiting visible blood contamination were excluded. SF MΦs were isolated and immunolabeled using a previously established protocol (Gómez-Aristizábal *et al.*, 2019). For the tolerization study, isolated SF MΦs were cultured in the presence or absence of lipopolysaccharide (LPS, 10 ng/mL) for 48h, and restimulation with 10 ng/ml LPS for 4h. Details of the antibodies used for MΦ immunophenotyping and intracellular staining are provided in Table S3.

Isolation of CD14^{+} monocytes and MSC(M)

Human peripheral blood mononuclear cells (PBMCs) were isolated from the whole blood of healthy donors (REB14-7483) or late-stage OA patients using density gradient centrifugation. $CD14^+$ monocytes were purified via magnetic sorting using CD14 MicroBeads (Miltenyi Biotec), following the manufacturer's protocol (George, Georgouli and Sanz-Moreno, 2022). $CD14^+$ monocytes were cryopreserved until use. $CD14^+$ monocytes were cultured in RPMI1640 medium supplemented with 10% fetal bovine serum, 1% sodium pyruvate, and 1% penicillin-streptomycin (Gibco). Each experimental condition included three independent biological donors with three technical replicates.

MSC(M) were isolated from bone marrow aspirates obtained from the iliac crest of healthy donors (REB 16-5493) and expanded as before (Gómez-Aristizábal, Kim and Viswanathan, 2016). MSC(M) were thawed three days before experiments at passage 4. MSC(M) were characterized as before (Gómez-Aristizábal *et al.*, 2017). Three biological donors were used (Table S1).

Evaluation of soluble factors in SF and cell culture medium by Enzyme-linked immunosorbent assay (ELISA)

Clear SF samples after centrifugation (12,000xg for 15 min) or conditioned medium (CM) were stored at -80ºC until analysis. IL-6, CCL2, S100A8/9, IL-6-sIL-6R, sIL-6R, IL-8 and TNF were detected using the ELISA kit manufacturer's instructions and diluted with kit-specific solutions (as detailed in Table S4). For TNF assays, cells were re-stimulated with LPS (*E. coli* origin, 2.5 ng/mL; Millipore-Sigma) for 4 hours before collecting the CM at 48h.

$CD14^+$ monocyte and MSC(M) culture and treatments

$CD14^+$ monocytes (2.5×10^5 cells) were cultured in 24-well plates in a total volume of 400 µL. $CD14^+$ monocytes were treated with human recombinant IL-6 at concentrations of 0.5, 5, 10, and 50 ng/mL (PeproTech, 200-06); S100A8/9 at 1 µg/mL (R&D Systems, B226-S8); sIL-6R (Cedar Lane, CLCYT286) at 10 ng/mL, and sgp130 (R&D Systems, 228-GP) at 10 ng/mL. Pooled mid- or late-stage OA SF, collected from eight patients, was used at 30% (v/v%) for each set of experiments. For inhibitors, $CD14^+$ monocytes were pre-treated for 1 hour with IL-6 neutralizing antibody (2.5 µg/mL; R&D Systems, MAB206), or TAK-242 (1 µM/mL; Millipore-Sigma, 5.08336), or SP600125 (50 nM/mL; Adooq Bioscience, A21502). Short-term exposure times were variable and consisted of $CD14^+$ monocytes treatment with recombinant IL-6 (5 ng/mL) or S100A8/9 (1 µg/mL) for 40 minutes, or with 30% (v/v) pooled late-stage OA SF for 1 hour. Long-term exposures consisted of the same stimuli for 24 hours (Fig. 4A).

$CD14^+$ monocytes were co-cultured directly with MSC(M) at a 5:1 ratio with indicated conditions for 72 hours. $CD14^+$ monocytes in co-cultures with MSC(M) were licensed with mid- or late-stage OA SF, with or without pre-treatment (for 1h) with IL-6 neutralizing antibody (Fig. 5A). Healthy or late-stage OA $CD14^+$ monocyte tolerization was assessed only via direct co-cultures with and without MSC(M) in late-stage OA SF for 72h, followed by additional 4-hour LPS re-challenge. Conditioned medium, termed as late OA SF licensed MSC(M) CM, containing soluble factors from these co-cultures, was centrifuged at 1,000g for 5 min and stored at −80 °C for subsequent use in secondary $CD14^+$ monocyte cultures for downstream analysis, including western blotting, gene and soluble TNF assessments (Fig. 6A).

MSC(M) were treated with late-OA SF for 1h, 24h, 48h and 72h, and the percentage of early apoptotic cells was subsequently assessed by flow cytometry. Cells were harvested using TrypLE (Gibco), followed by staining with the Annexin V-FITC Apoptosis Detection Kit with 7-AAD (Biolegend, Cat# 640922), according to the manufacturer's instructions. Early apoptosis was determined as the percentage of Annexin V^+ within the live, 7-AAD-negative MSC(M).

$CD14^+$ monocytes flow cytometry

For flow cytometric analysis, $CD14^+$ monocytes were harvested after 72 hours of treatment, washed with sterile phosphate-buffered saline (PBS) and immunolabeled with antibodies against CD45, CD14, CD16, and either CD163, CD206, HLA-DR, CD86, or mIL-6R, as listed in Table S3. $CD45^+$ monocytes were classified based on the expression of CD14 and CD16 (Fig. S2A). The MFI was quantified using FlowJo analysis software version 10.10. The MFI of each cell surface marker on treated $CD14^+$ monocytes was normalized to the donor-matched average MFI value of the corresponding marker measured in three technical replicates of untreated $CD14^+$ monocytes. Normalized MFI values from three biological replicates were analyzed across different treatment conditions.

Western blot analysis

$CD14^+$ monocytes cultured for short and longer-term exposures (Fig. 4A and 6A) were lysed using standard protocols (Waise *et al.*, 2019). 15 µg of cell lysates were subjected to electrophoresis on a 10% polyacrylamide gel and transferred to polyvinylidene fluoride (PVDF) membranes. Membranes were blocked and immunoblotted with indicated primary antibodies (Table S5), diluted 1000-fold. The blots were washed with Tris-based

saline-tween 20 (TBS-T) and incubated with secondary horseradish peroxidase (HRP)-conjugated antibodies (Cell Signaling) in 5% skim milk. After washing the membranes in TBS-T, the signal was detected with the enhanced chemiluminescence reagent (ThermoFisher Scientific) and a Bio-Rad chemiluminescent imaging system. The images were quantified with ImageJ analysis software. Phosphorylated kinases were normalized for glyceraldehyde-3-phosphate dehydrogenase (GAPDH) or corresponding total protein.

Gene expression analysis

After 48h of exposure under indicated conditions, $CD14^+$ monocytes were collected for gene expression readouts. Total RNA from treated $CD14^+$ monocytes was extracted with TRI zol reagent (Life Technologies). cDNA was synthesized using SuperScript IV VILO master mix (ThermoFisher Scientific) per the manufacturer's instructions. The primer sequences are listed (Table S6). A PCR detection system (Q5; ThermoFisher Scientific) with the following cycling parameters: initial denaturation at 95 °C for 60 s, followed by 40 cycles of 95°C for 10 s and 60°C for 30s was used. The levels of target mRNA were normalized to three housekeeping mRNA levels of GAPDH, beta-2-microglobulin (B2M) and β-Actin using the $2^{-\Delta\Delta Ct}$ method.

Phagocytosis

$CD14^+$ monocytes were differentiated into macrophages over 5 days in the presence of 20 ng/mL M-CSF (PeproTech). Macrophages (1×10^5 cells per well) were seeded in 96-well plates and treated for an additional 3 days with M-CSF (20 ng/mL), with or without either late-stage OA SF, or CM from late-stage OA SF licensed MSC(M), in the presence or absence of IL-6 neutralizing antibody. Following 3 days of treatment, cells were washed with PBS, and phagocytosis of pHrodo™ Deep Red E. coli BioParticles® Conjugate

(ThermoFisher Scientific, P35360) was assessed according to the manufacturer's protocol.

The particles were diluted 1:10 in 100 µL cell culture medium to achieve a final concentration of 10 µg/mL. Cells were incubated at 37°C for 1 hour, and fluorescence was measured using a plate reader with excitation and emission settings of 640 ± 15 nm and 690 ± 20 nm, respectively.

Proteome profiler array

The phosphorylation of protein kinases in $CD14^+$ monocytes treated with late-stage OA SF for 1 hour was assessed using the Human Phospho-Kinase Array Kit (R&D Systems; ARY003C), according to the manufacturer's instructions. The array detects phosphorylation at 37 kinase-specific sites. Signal intensities, representing the relative levels of phosphorylated proteins bound to each pair of duplicate spots, were quantified using ImageJ analysis software.

Statistical analysis

Statistical and graphical analyses were performed using Prism (GraphPad) and JMP Pro 18 (SAS). Normality tests were conducted prior to each analysis (significance level set at $p < 0.05$). *In vitro* data met normality tests. Parametric data from *in vitro* assays were analyzed using ordinary one-way ANOVA with Tukey's multiple comparisons test. For non-parametric data, including soluble factor concentrations and immunophenotyping of MΦs in SF of OA patients, Kruskal-Wallis test with Dunn's multiple comparisons test was applied. A p-value of < 0.05 was considered statistically significant.

Supplemental material includes Fig. S1-S5 and Tables S1-S6.

Acknowledgements

This work is supported by the Arthritis Society (YIO-15-321) and CIHR (PJT-166089) to SV. The work is in part supported by the Schroeder Arthritis Institute via the Toronto General and Western Hospital Foundation (University Health Network). We thank the UHN Biobank, led by Mohit Kapoor and team, specifically Kim Perry, Christina Ward, and Luis Montoya from the Arthritis program, for their work in SF sample management, consent, and data collection. Dr. Vinod Chandran for providing psoriatic and rheumatoid arthritis SF samples. Schematics were developed using BioRender.com.

Author Contributions

Methodology, investigation, formal analysis and visualization, MR. Methodology, ABF. Writing original draft, formal analysis and visualization, KR. Resources, RG. Conceptualization, writing, original draft and editing, supervision, project administration, fund acquisition, SV.

Declaration of interests

SV has 60% ownership of a regulatory consulting company, which does not conflict with the work done here. MR, ABF, RG declare no conflicts. KR is currently employed by Stem Cell Technologies.

References

Ahmed, R., Soliman, N. and Elwan, S. (2023) ‘Relationships between Serum Interleukin-6, Radiographic Severity a WOMAC Index in Patients with Primary Knee Osteoarthritis’, *The Egyptian Journal of Hospital Medicine*, 92(1), pp. 6082–6086. Available at: https://doi.org/10.21608/ejhm.2023.312355.

Amin, A.R. *et al.* (1997) ‘Superinduction of cyclooxygenase-2 activity in human osteoarthritis-affected cartilage. Influence of nitric oxide’, *The Journal of Clinical Investigation*, 99(6), pp. 1231–1237. Available at: https://doi.org/10.1172/JCI119280.

Assirelli, E. *et al.* (2020) ‘Complement Expression and Activation in Osteoarthritis Joint Compartments’, *Frontiers in Immunology*, 11, p. 535010. Available at: https://doi.org/10.3389/fimmu.2020.535010.

Babon, J.J., Varghese, L.N. and Nicola, N.A. (2014) ‘Inhibition of IL-6 family cytokines by SOCS3’, *Seminars in immunology*, 26(1), pp. 13–19. Available at: https://doi.org/10.1016/j.smim.2013.12.004.

Bauer, J. *et al.* (1989) ‘Regulation of interleukin 6 receptor expression in human monocytes and monocyte-derived macrophages. Comparison with the expression in human hepatocytes’, *The Journal of Experimental Medicine*, 170(5), pp. 1537–1549. Available at: https://doi.org/10.1084/jem.170.5.1537.

Bennett, B.L. *et al.* (2001) ‘SP600125, an anthrapyrazolone inhibitor of Jun N-terminal kinase’, *Proceedings of the National Academy of Sciences of the United States of America*, 98(24), pp. 13681–13686. Available at: https://doi.org/10.1073/pnas.251194298.

Bouffi, C. *et al.* (2010) ‘IL-6-dependent PGE2 secretion by mesenchymal stem cells inhibits local inflammation in experimental arthritis’, *PloS One*, 5(12), p. e14247. Available at: https://doi.org/10.1371/journal.pone.0014247.

Chahal, J. *et al.* (2019) ‘Bone Marrow Mesenchymal Stromal Cell Treatment in Patients with Osteoarthritis Results in Overall Improvement in Pain and Symptoms and Reduces Synovial Inflammation’, *Stem Cells Translational Medicine*, 8(8), pp. 746–757. Available at: https://doi.org/10.1002/sctm.18-0183.

Chen, W.-C. *et al.* (2019) ‘Resistin Enhances Monocyte Chemoattractant Protein-1 Production in Human Synovial Fibroblasts and Facilitates Monocyte Migration | Cell Physiol Biochem’, *Cellular Physiology & Biochemistry*, 52(3), pp. 408–420.

Chomarat, P. *et al.* (2000) ‘IL-6 switches the differentiation of monocytes from dendritic cells to macrophages’, *Nature Immunology*, 1(6), pp. 510–514. Available at: https://doi.org/10.1038/82763.

Copp, G., Robb, K.P. and Viswanathan, S. (2023) ‘Culture-expanded mesenchymal stromal cell therapy: does it work in knee osteoarthritis? A pathway to clinical success’, *Cellular & Molecular Immunology*, 20(6), pp. 626–650. Available at: https://doi.org/10.1038/s41423-023-01020-1.

Del Sordo, L. *et al.* (2023) ‘Impaired Efferocytosis by Synovial Macrophages in Patients With Knee Osteoarthritis’, *Arthritis & Rheumatology (Hoboken, N.J.)*, 75(5), pp. 685–696. Available at: https://doi.org/10.1002/art.42412.

Delprat, V. *et al.* (2020) ‘Cycling hypoxia promotes a pro-inflammatory phenotype in macrophages via JNK/p65 signaling pathway’, *Scientific Reports*, 10(1), p. 882. Available at: https://doi.org/10.1038/s41598-020-57677-5.

Evans, C. (2018) ‘Arthritis Gene Therapy using the Interleukin-1 Receptor Antagonist’, *Arthritis & rheumatology (Hoboken, N.J.)*, 70(11), pp. 1699–1701. Available at: https://doi.org/10.1002/art.40675.

Fumeaux, T. and Pugin, J. (2002) ‘Role of Interleukin-10 in the Intracellular Sequestration of Human Leukocyte Antigen-DR in Monocytes during Septic Shock’, *American Journal of Respiratory and Critical Care Medicine*, 166(11), pp. 1475–1482. Available at: https://doi.org/10.1164/rccm.200203-217OC.

Galleu, A. *et al.* (2017) ‘Apoptosis in mesenchymal stromal cells induces in vivo recipient-mediated immunomodulation’, *Science Translational Medicine*, 9(416), p. eaam7828. Available at: https://doi.org/10.1126/scitranslmed.aam7828.

George, S., Georgouli, M. and Sanz-Moreno, V. (2022) ‘Protocol to drive human monocyte-to-macrophage polarization *in vitro* using tumor conditioned media’, *STAR Protocols*, 3(4), p. 101666. Available at: https://doi.org/10.1016/j.xpro.2022.101666.

Gobezie, R. *et al.* (2007) ‘High abundance synovial fluid proteome: distinct profiles in health and osteoarthritis’, *Arthritis Research & Therapy*, 9(2), p. R36. Available at: https://doi.org/10.1186/ar2172.

Gómez-Aristizábal, A. *et al.* (2017) ‘Stage-specific differences in secretory profile of mesenchymal stromal cells (MSCs) subjected to early- vs late-stage OA synovial fluid’, *Osteoarthritis and Cartilage*, 25(5), pp. 737–741. Available at: https://doi.org/10.1016/j.joca.2016.11.010.

Gómez-Aristizábal, A. *et al.* (2019) ‘Synovial fluid monocyte/macrophage subsets and their correlation to patient-reported outcomes in osteoarthritic patients: a cohort study’, *Arthritis Research & Therapy*, 21(1), p. 26. Available at: https://doi.org/10.1186/s13075-018-1798-2.

Gómez-Aristizábal, A., Kim, K.-P. and Viswanathan, S. (2016) ‘A Systematic Study of the Effect of Different Molecular Weights of Hyaluronic Acid on Mesenchymal Stromal

Cell-Mediated Immunomodulation', *PLOS ONE*, 11(1), p. e0147868. Available at: https://doi.org/10.1371/journal.pone.0147868.

Gu, J.-Y. *et al.* (2022) 'Endotoxin tolerance induced by *Porphyromonas gingivalis* lipopolysaccharide alters macrophage polarization', *Microbial Pathogenesis*, 164, p. 105448. Available at: https://doi.org/10.1016/j.micpath.2022.105448.

Hamilton, A.M. *et al.* (2019) 'Iron nanoparticle-labeled murine mesenchymal stromal cells in an osteoarthritic model persists and suggests anti-inflammatory mechanism of action', *PloS One*, 14(12), p. e0214107. Available at: https://doi.org/10.1371/journal.pone.0214107.

Han, M.S. *et al.* (2012) 'JNK Expression by Macrophages Promotes Obesity-induced Insulin Resistance and Inflammation', *Science (New York, N.Y.)*, 339(6116), p. 10.1126/science.1227568. Available at: https://doi.org/10.1126/science.1227568.

Heinrich, P.C. *et al.* (2003) 'Principles of interleukin (IL)-6-type cytokine signalling and its regulation.', *Biochemical Journal*, 374(Pt 1), pp. 1–20. Available at: https://doi.org/10.1042/BJ20030407.

Hibi, M. *et al.* (1990) 'Molecular cloning and expression of an IL-6 signal transducer, gp130', *Cell*, 63(6), pp. 1149–1157. Available at: https://doi.org/10.1016/0092-8674(90)90411-7.

Huang, Z.Y. *et al.* (2016) 'Both systemic and local lipopolysaccharide (LPS) burden are associated with knee OA severity and inflammation', *Osteoarthritis and Cartilage*, 24(10), pp. 1769–1775. Available at: https://doi.org/10.1016/j.joca.2016.05.008.

Huber, R. *et al.* (2017) 'TNF Tolerance in Monocytes and Macrophages: Characteristics and Molecular Mechanisms', *Journal of Immunology Research*, 2017, p. 9570129. Available at: https://doi.org/10.1155/2017/9570129.

Ii, M. *et al.* (2006) 'TAK-242, a novel Toll-like receptor 4 signal transduction inhibitor, protects mice in Escherichia coli-induced and lipoteichoic acid-induced lethality models', *Critical Care*, 10(1), p. P153. Available at: https://doi.org/10.1186/cc4500.

Iijima, H. *et al.* (2018) 'Effectiveness of mesenchymal stem cells for treating patients with knee osteoarthritis: a meta-analysis toward the establishment of effective regenerative rehabilitation', *NPJ Regenerative medicine*, 3, p. 15. Available at: https://doi.org/10.1038/s41536-018-0041-8.

Karin, M. and Ben-Neriah, Y. (2000) 'Phosphorylation meets ubiquitination: the control of NF-[kappa]B activity', *Annual Review of Immunology*, 18, pp. 621–663. Available at: https://doi.org/10.1146/annurev.immunol.18.1.621.

Kim, J. and Hematti, P. (2009) 'Mesenchymal stem cell–educated macrophages: A novel type of alternatively activated macrophages', *Experimental Hematology*, 37(12), pp. 1445–1453. Available at: https://doi.org/10.1016/j.exphem.2009.09.004.

Kim, Y.E. *et al.* (2023) ‘SOCS3 Protein Mediates the Therapeutic Efficacy of Mesenchymal Stem Cells against Acute Lung Injury’, *International Journal of Molecular Sciences*, 24(9), p. 8256. Available at: https://doi.org/10.3390/ijms24098256.

Kishimoto, T., Akira, S. and Taga, T. (1992) ‘Interleukin-6 and its receptor: a paradigm for cytokines’, *Science (New York, N.Y.)*, 258(5082), pp. 593–597. Available at: https://doi.org/10.1126/science.1411569.

Kishimoto, T., Kang, S. and Tanaka, T. (2015) ‘IL-6: A New Era for the Treatment of Autoimmune Inflammatory Diseases’, in K. Nakao, N. Minato, and S. Uemoto (eds) *Innovative Medicine: Basic Research and Development*. Tokyo: Springer. Available at: http://www.ncbi.nlm.nih.gov/books/NBK500320/ (Accessed: 21 January 2025).

Kraus, V.B. *et al.* (2016) ‘Direct in vivo evidence of activated macrophages in human osteoarthritis’, *Osteoarthritis and Cartilage*, 24(9), pp. 1613–1621. Available at: https://doi.org/10.1016/j.joca.2016.04.010.

Li, L. *et al.* (2020) ‘Profiling of inflammatory mediators in the synovial fluid related to pain in knee osteoarthritis’, *BMC Musculoskeletal Disorders*, 21(1), p. 99. Available at: https://doi.org/10.1186/s12891-020-3120-0.

Li, M. *et al.* (2011) ‘NFκB and JNK/MAPK activation mediates the production of major macrophage- or dendritic cell-recruiting chemokine in human first trimester decidual cells in response to proinflammatory stimuli’, *The Journal of Clinical Endocrinology and Metabolism*, 96(8), pp. 2502–2511. Available at: https://doi.org/10.1210/jc.2011-0055.

Li, X. *et al.* (2009) ‘PGE2 And Its Cognate EP Receptors Control Human Adult Articular Cartilage Homeostasis and Are Linked to the Pathophysiology of Osteoarthritis’, *Arthritis and rheumatism*, 60(2), pp. 513–523. Available at: https://doi.org/10.1002/art.24258.

Liu, F.-B., Lin, Q. and Liu, Z.-W. (2016) ‘A study on the role of apoptotic human umbilical cord mesenchymal stem cells in bleomycin-induced acute lung injury in rat models’, *European Review for Medical and Pharmacological Sciences*, 20(5), pp. 969–982.

Livshits, G. *et al.* (2009) ‘Interleukin-6 is a significant predictor of radiographic knee osteoarthritis: The Chingford study’, *Arthritis and Rheumatism*, 60(7), p. 2037. Available at: https://doi.org/10.1002/art.24598.

Lust, J.A. *et al.* (1992) ‘Isolation of an mRNA encoding a soluble form of the human interleukin-6 receptor’, *Cytokine*, 4(2), pp. 96–100. Available at: https://doi.org/10.1016/1043-4666(92)90043-q.

Lv, H. *et al.* (2020) ‘Mesenchymal stromal cells ameliorate acute lung injury induced by LPS mainly through stanniocalcin-2 mediating macrophage polarization’, *Annals of Translational Medicine*, 8(6), pp. 334–334. Available at: https://doi.org/10.21037/atm.2020.02.105.

Maekawa, A. *et al.* (2021) ‘Prostaglandin E2 induces dual-specificity phosphatase-1, thereby attenuating inflammatory genes expression in human osteoarthritic synovial fibroblasts’, *Prostaglandins & Other Lipid Mediators*, 154, p. 106550. Available at: https://doi.org/10.1016/j.prostaglandins.2021.106550.

Matas, J. *et al.* (2019) ‘Umbilical Cord-Derived Mesenchymal Stromal Cells (MSCs) for Knee Osteoarthritis: Repeated MSC Dosing Is Superior to a Single MSC Dose and to Hyaluronic Acid in a Controlled Randomized Phase I/II Trial’, *Stem Cells Translational Medicine*, 8(3), pp. 215–224. Available at: https://doi.org/10.1002/sctm.18-0053.

Mathiessen, A. and Conaghan, P.G. (2017) ‘Synovitis in osteoarthritis: current understanding with therapeutic implications’, *Arthritis Research & Therapy*, 19(1), p. 18. Available at: https://doi.org/10.1186/s13075-017-1229-9.

Metcalf, T.U. *et al.* (2017) ‘Human monocyte subsets are transcriptionally and functionally altered in aging in response to pattern recognition receptor agonists’, *Journal of immunology (Baltimore, Md. : 1950)*, 199(4), pp. 1405–1417. Available at: https://doi.org/10.4049/jimmunol.1700148.

Midwood, K. *et al.* (2009) ‘Tenascin-C is an endogenous activator of Toll-like receptor 4 that is essential for maintaining inflammation in arthritic joint disease’, *Nature Medicine*, 15(7), pp. 774–780. Available at: https://doi.org/10.1038/nm.1987.

Mikulkova, Z. *et al.* (2024) ‘Complexity of synovial fluid-derived monocyte-macrophage-lineage cells in knee osteoarthritis’, *Cell Reports*, 43(12), p. 115011. Available at: https://doi.org/10.1016/j.celrep.2024.115011.

Mittal, M. *et al.* (2016) ‘TNFα-stimulated gene-6 (TSG6) activates macrophage phenotype transition to prevent inflammatory lung injury’, *Proceedings of the National Academy of Sciences*, 113(50), pp. E8151–E8158. Available at: https://doi.org/10.1073/pnas.1614935113.

Nordan, R.P. and Potter, M. (1986) ‘A Macrophage-Derived Factor Required by Plasmacytomas for Survival and Proliferation in Vitro’, *Science*, 233(4763), pp. 566–569. Available at: https://doi.org/10.1126/science.3726549.

Özler, K. *et al.* (2016) ‘Serum and knee synovial fluid matrix metalloproteinase-13 and tumor necrosis factor-alpha levels in patients with late-stage osteoarthritis’, *Acta Orthopaedica Et Traumatologica Turcica*, 50(3), pp. 356–361. Available at: https://doi.org/10.3944/AOTT.2015.15.0115.

Prieto-Potin, I. *et al.* (2015) ‘Characterization of multinucleated giant cells in synovium and subchondral bone in knee osteoarthritis and rheumatoid arthritis’, *BMC musculoskeletal disorders*, 16, p. 226. Available at: https://doi.org/10.1186/s12891-015-0664-5.

Prockop, D.J. (2016) ‘Inflammation, fibrosis, and modulation of the process by mesenchymal stem/stromal cells’, *Matrix Biology: Journal of the International Society for Matrix Biology*, 51, pp. 7–13. Available at: https://doi.org/10.1016/j.matbio.2016.01.010.

Reeh, H. *et al.* (2019) ‘Response to IL-6 trans- and IL-6 classic signalling is determined by the ratio of the IL-6 receptor α to gp130 expression: fusing experimental insights and dynamic modelling’, *Cell Communication and Signaling : CCS*, 17, p. 46. Available at: https://doi.org/10.1186/s12964-019-0356-0.

Richette, P. *et al.* (2021) ‘Efficacy of tocilizumab in patients with hand osteoarthritis: double blind, randomised, placebo-controlled, multicentre trial’, *Annals of the Rheumatic Diseases*, 80(3), pp. 349–355. Available at: https://doi.org/10.1136/annrheumdis-2020-218547.

Riethmueller, S. *et al.* (2017) ‘Proteolytic Origin of the Soluble Human IL-6R In Vivo and a Decisive Role of N-Glycosylation’, *PLoS biology*, 15(1). Available at: https://doi.org/10.1371/journal.pbio.2000080.

Rogacev, K.S. *et al.* (2012) ‘CD14++CD16+ Monocytes Independently Predict Cardiovascular Events: A Cohort Study of 951 Patients Referred for Elective Coronary Angiography’, *Journal of the American College of Cardiology*, 60(16), pp. 1512–1520. Available at: https://doi.org/10.1016/j.jacc.2012.07.019.

Roos, E.M. *et al.* (1998) *Knee injury and Osteoarthritis Outcome Score (KOOS)*, *ePROVIDE - Mapi Research Trust*. Available at: https://eprovide.mapi-trust.org/instruments/knee-injury-and-osteoarthritis-outcome-score.

Rose-John, S. (2017) ‘The Soluble Interleukin 6 Receptor: Advanced Therapeutic Options in Inflammation’, *Clinical Pharmacology & Therapeutics*, 102(4), pp. 591–598. Available at: https://doi.org/10.1002/cpt.782.

Rose-John, S. and Heinrich, P.C. (1994) ‘Soluble receptors for cytokines and growth factors: generation and biological function’, *Biochemical Journal*, 300(2), pp. 281–290. Available at: https://doi.org/10.1042/bj3000281.

Russo, A. *et al.* (2022) ‘Alarming and Calming: Opposing Roles of S100A8/S100A9 Dimers and Tetramers on Monocytes’, *Advanced Science*, 9(36), p. 2201505. Available at: https://doi.org/10.1002/advs.202201505.

Ryu, J.-H. *et al.* (2011) ‘Interleukin-6 plays an essential role in hypoxia-inducible factor 2α-induced experimental osteoarthritic cartilage destruction in mice’, *Arthritis and Rheumatism*, 63(9), pp. 2732–2743. Available at: https://doi.org/10.1002/art.30451.

Shalova, I.N. *et al.* (2015) ‘Human Monocytes Undergo Functional Re-programming during Sepsis Mediated by Hypoxia-Inducible Factor-1α’, *Immunity*, 42(3), pp. 484–498. Available at: https://doi.org/10.1016/j.immuni.2015.02.001.

Smith, M.D. *et al.* (1997) ‘Synovial membrane inflammation and cytokine production in patients with early osteoarthritis’, *The Journal of Rheumatology*, 24(2), pp. 365–371.

Sowers, M. *et al.* (2011) ‘Associations of Anatomical Measures from MRI with Radiographically Defined Knee Osteoarthritis Score, Pain, and Physical Functioning’, *JBJS*, 93(3), p. 241. Available at: https://doi.org/10.2106/JBJS.I.00667.

Steinmetz, J.D. *et al.* (2023) ‘Global, regional, and national burden of osteoarthritis, 1990–2020 and projections to 2050: a systematic analysis for the Global Burden of Disease Study 2021’, *The Lancet Rheumatology*, 5(9), pp. e508–e522. Available at: https://doi.org/10.1016/S2665-9913(23)00163-7.

Sung, P.-H. *et al.* (2013) ‘Apoptotic adipose-derived mesenchymal stem cell therapy protects against lung and kidney injury in sepsis syndrome caused by cecal ligation puncture in rats’, *Stem Cell Research & Therapy*, 4(6), p. 155. Available at: https://doi.org/10.1186/scrt385.

Vogl, T. *et al.* (2007) ‘Mrp8 and Mrp14 are endogenous activators of Toll-like receptor 4, promoting lethal, endotoxin-induced shock’, *Nature Medicine*, 13(9), pp. 1042–1049. Available at: https://doi.org/10.1038/nm1638.

Waise, T.M.Z. *et al.* (2019) ‘Inhibition of upper small intestinal mTOR lowers plasma glucose levels by inhibiting glucose production’, *Nature Communications*, 10(1), p. 714. Available at: https://doi.org/10.1038/s41467-019-08582-7.

Wang, C. *et al.* (2024) ‘Transcriptomic profiling of osteoarthritis synovial macrophages reveals a tolerized phenotype compounded by a weak corticosteroid response’, *Rheumatology (Oxford, England)*, 64(2), pp. 860–869. Available at: https://doi.org/10.1093/rheumatology/keae161.

Wang, L. *et al.* (2003) ‘IL-6 Induces NF-κB Activation in the Intestinal Epithelia 1’, *The Journal of Immunology*, 171(6), pp. 3194–3201. Available at: https://doi.org/10.4049/jimmunol.171.6.3194.

Wang, W. *et al.* (2024) ‘Chemokine CCL2 promotes cardiac regeneration and repair in myocardial infarction mice via activation of the JNK/STAT3 axis’, *Acta Pharmacologica Sinica*, 45(4), pp. 728–737. Available at: https://doi.org/10.1038/s41401-023-01198-0.

Wei, X. *et al.* (2024) ‘Circ-phkb promotes cell apoptosis and inflammation in LPS-induced alveolar macrophages via the TLR4/MyD88/NF-kB/CCL2 axis’, *Respiratory Research*, 25(1), p. 62. Available at: https://doi.org/10.1186/s12931-024-02677-6.

Wiegertjes, R., Loo, F.A.J. van de and Davidson, E.N.B. (2020) ‘A roadmap to target interleukin-6 in osteoarthritis’, *Rheumatology (Oxford, England)*, 59(10), p. 2681. Available at: https://doi.org/10.1093/rheumatology/keaa248.

Wu, X. *et al.* (2018) 'Interleukin-6 from subchondral bone mesenchymal stem cells contributes to the pathological phenotypes of experimental osteoarthritis', *American Journal of Translational Research*, 10(4), pp. 1143–1154.

Yan, J. *et al.* (2020) 'Reduced IκB-α Protein Levels in Peripheral Blood Cells of Patients with Multiple Sclerosis—A Possible Cause of Constitutive NF-κB Activation', *Journal of Clinical Medicine*, 9(8), p. 2534. Available at: https://doi.org/10.3390/jcm9082534.

Yasukawa, H. *et al.* (2003) 'IL-6 induces an anti-inflammatory response in the absence of SOCS3 in macrophages', *Nature Immunology*, 4(6), pp. 551–556. Available at: https://doi.org/10.1038/ni938.

Yin, Q. *et al.* (2022) 'The CD14++CD16+ monocyte subset is expanded and controls Th1 cell development in Graves' disease', *Clinical Immunology*, 245, p. 109160. Available at: https://doi.org/10.1016/j.clim.2022.109160.

Yu, L. *et al.* (2023) 'Efficacy and safety of anti-interleukin-1 therapeutics in the treatment of knee osteoarthritis: a systematic review and meta-analysis of randomized controlled trials', *Journal of Orthopaedic Surgery and Research*, 18, p. 100. Available at: https://doi.org/10.1186/s13018-023-03590-2.

Zhang, C. *et al.* (2017) 'Tumor necrosis factor alpha-stimulated gene-6 (TSG-6) inhibits the inflammatory response by inhibiting the activation of P38 and JNK signaling pathway and decreases the restenosis of vein grafts in rats', *Heart and Vessels*, 32(12), pp. 1536–1545. Available at: https://doi.org/10.1007/s00380-017-1059-3.

Zhang, Y. *et al.* (2011) 'Fluctuation of knee pain and changes in bone marrow lesions, effusions, and synovitis on magnetic resonance imaging', *Arthritis and Rheumatism*, 63(3), pp. 691–699. Available at: https://doi.org/10.1002/art.30148.

Zhang, Y. *et al.* (2023) 'CC chemokines and receptors in osteoarthritis: new insights and potential targets', *Arthritis Research & Therapy*, 25, p. 113. Available at: https://doi.org/10.1186/s13075-023-03096-6.

Figure legends

Figure 1. OA synovial fluid contains different cytokines, chemokines and MΦ subsets displaying mixed phenotypes

(A-D) Median and interquartile range of IL-6, chemokine (C-C motif) ligand 2 (CCL2), S100A8/9, and IL-8 concentrations in synovial fluid (SF) samples from not OA SF (Not OA; N=6-11); mid-stage OA SF (Mid OA; N=21-30); late-stage OA SF (Late OA; N=29-

35). **(E)** Frequency of MΦ subsets in the late-OA SF. **(F-I)** The mean fluorescence intensity (MFI) expression of CD163, CD206, HLA-DR, and HLA-DR/CD163 MFI expression ratio, in late-OA SF MΦ subsets (N=25-43). **(J)** Immunophenotyping, intracellular IL-1β and TNF evaluation of late-OA SF MΦ following stimulation with lipopolysaccharides (LPS, 10 ng/mL; N=4). Kruskal-Wallis test with Dunn's multiple comparisons test was used (*$p<0.05$; ** $p< 0.001$; ***$p<0.0001$; **** $p< 0.00001$).

Figure 2. Exposure of peripheral CD14$^+$ monocytes to late-OA SF partially increased the frequency of the intermediate monocyte subset and partially tolerized them

(A) Frequency of classical (CD14$^+$CD16^{neg}) and intermediate (CD14$^+$CD16$^+$) peripheral CD14$^+$ monocyte subsets with and without OA synovial fluid (SF). **(B)** Percent intermediate (CD14$^+$CD16$^+$) monocytes in CD45$^+$ cells with indicated treatments. **(C, D)** Mean fluorescence intensity (MFI) of CD163, CD206, HLA-DR, and CD86 surface markers, and HLA-DR/CD163 MFI ratio on peripheral CD14$^+$ monocytes from late-OA patients and healthy donors, with or without late-stage OA SF, following lipopolysaccharides (LPS, 2.5 ng/mL) stimulation. **(E-I)** MFI expression of CD163, CD206, HLA-DR, and CD86 cell surface markers and HLA-DR/CD163 MFI expression ratio on healthy peripheral CD14$^+$ monocytes at the indicated conditions. **(J)** Tumor necrosis factor (TNF) soluble factor production by peripheral CD14$^+$ monocytes in indicated treatments, with LPS (2.5 ng/mL) stimulation. Peripheral CD14$^+$ monocytes were cultured for 72h with indicated treatments in (A-I) for flow cytometry assay and 48 hours in (J) for TNF assay; IL-6 recombinant (5 ng/mL); IL-6 neutralizing antibody (Ab; 2.5 µg/mL); 30%

pooled mid- or late-OA SF. Values are shown as mean ± SD; N=3 biological replicates; n ≥ 3 technical replicates. An ordinary one-way ANOVA with Tukey's multiple comparisons test was used. Letters indicate significant differences ($p < 0.05$) between groups; asterisks indicate significance ($p<0.05$) relative to untreated controls.

Figure 3. Physiological levels of IL-6 in OA SF signal through classical, not trans-signaling

(A) Schematic representation of dual IL-6 signaling in cells such as monocytes/macrophages (MΦs) expressing IL-6 receptor (IL-6R): i) trans-signaling through glycoprotein (gp)130 and soluble IL-6R (sIL-6R shed by a disintegrin and metalloproteinase 17 (ADAM 17)); ii) classical signaling through membrane-bound (m) IL-6R and gp130. **(B)** Median and interquartile range of sIL-6R concentration in synovial fluid (SF) samples from not-OA (N=7); mid-OA (N=24); and late-OA (N=43). **(C-F)** Mean fluorescence intensity (MFI) expression of CD163, CD206, HLA-DR and CD86 cell surface markers in the presence of late-OA SF and physiological levels of IL-6 (0.5 ng/mL) or/and sIL-6R (10 ng/mL), soluble(s) gp130 (10 ng/mL). **(G)** mIL-6R expression on $CD14^+$ monocytes at the indicated treatments. **(H)** IL-6: sIL-6R complex levels in not-OA SF (N=7); mid-OA SF (N=24); late-OA SF (N=72), psoriatic arthritis (PsA) SF (N=2) and rheumatoid arthritis (RA) SF (N=1). Peripheral $CD14^+$ monocytes were cultured for 72h with 30% pooled mid- or late-OA SFs, IL-6 neutralizing antibody (Ab; 2.5 µg/mL), and indicated treatments. MFI expression of monocyte cell surface markers is shown as mean ± SD; N=3 biological replicates; n=3 technical replicates. An ordinary one-way ANOVA with Tukey's multiple comparisons test was used. Letters indicate significant differences

($p < 0.05$) between groups; asterisks indicate significance ($p<0.05$) relative to untreated controls.

Figure 4. Late-OA SF stimulated multiple signaling pathways in CD14$^+$ monocytes, partially replicated by IL-6 and S100A8/9 stimulation

(A) An experimental timeline for CD14$^+$ monocytes indicating treatment conditions at each time point (arrows) for both short- and long-term exposure periods. **(B)** Representative western blot images from CD14$^+$ monocytes at short treatment exposures. **(C)** Representative western blot images from CD14$^+$ monocytes at long treatment exposures. **(D-F)** Bar graphs illustrating phosphorylated-signal transducer and activator of transcription 3 (p-STAT3), phosphorylated-c-Jun terminal kinase (p-JNK), and nuclear factor of kappa light polypeptide gene enhancer in B-cells inhibitor alpha (IκBα) levels (normalized to total glyceraldehyde-3-phosphate dehydrogenase; GAPDH) in short and long treatment exposures. **(G)** Suppressor of cytokine signaling 3 (*SOCS3*) expression in CD14$^+$ monocytes with indicated treatments. **(H)** Chemokine (C-C motif) ligand 2 (*CCL2*) expression in CD14$^+$ monocytes with indicated treatments. **(I)** Tumor necrosis factor (*TNF*) expression by CD14$^+$ monocytes in indicated treatments and lipopolysaccharides (2.5 ng/mL) stimulation. Peripheral CD14$^+$ monocytes were cultured for 48h (G-I); IL-6 recombinant (5 ng/mL); S100A8/9 recombinant (1 µg/mL); IL-6 neutralizing antibody (Ab; 2.5 µg/mL); 30% pooled late-OA synovial fluid (SF); TAK242 (1 µM/mL). Values are shown as mean ± SD; N=3 biological replicates; n≤3 technical replicates. An ordinary one-way ANOVA with Tukey's multiple comparisons test was used. Letters indicate

significant differences ($p < 0.05$) between groups; asterisks indicate significance ($p<0.05$) relative to untreated controls.

Figure 5. Direct co-culture of MSC(M) with CD14$^+$ monocytes further immunosuppressed them even in late-OA SF

(A) Experimental timeline and schematic workflow for CD14$^+$ monocytes directly co-cultured with MSC(M), 30% pooled mid- or late-OA synovial fluid (SF) or IL-6 neutralizing antibody (Ab; 2.5 µg/mL) for 72h. **(B-F)** Mean fluorescence intensity (MFI) expression of CD163, CD206, HLA-DR, CD86 cell surface markers and the ratio of HLA-DR/CD163 MFI expression on CD14$^+$ monocytes directly co-cultured with MSC(M) and indicated treatments. Values are shown as mean ± SD; N=3 biological replicates; n≤3 technical replicates. An ordinary one-way ANOVA with Tukey's multiple comparisons test was used. Letters indicate significant differences ($p<0.05$) between groups; asterisks indicate significance ($p<0.05$) relative to untreated controls.

Figure 6. Soluble Factors from licensed MSC(M) CM in late-stage OA environment attenuated pro-inflammatory signaling kinases, functionality, and activated downstream effector genes in CD14$^+$ monocytes

(A) Experimental timeline and schematic workflow for CD14$^+$ monocytes treated with soluble factors from licensed MSC(M) CM in OA environment for the indicated times. **(B)** Representative western blot images. **(C-E)** Bar graphs illustrating phosphorylated-signal transducer and activator of transcription 3 (p-STAT3), phosphorylated-c-Jun terminal kinase (p-JNK), and nuclear factor of kappa light polypeptide gene enhancer in B-cells

inhibitor alpha (IκBα) levels (normalized to total glyceraldehyde-3-phosphate dehydrogenase; GAPDH) after 24h of treatments. **(F)** Expression of the suppressor of cytokine signaling 3 (*SOCS3)* gene in treated $CD14^+$ monocytes. **(G and H)** JNK downstream chemokine (C-C motif) ligand 2 (*CCL2)* and tumor necrosis factor (*TNF)* genes expression in treated $CD14^+$ monocytes. **(I)** TNF soluble factor production by peripheral $CD14^+$ monocytes in indicated treatments and lipopolysaccharides (2.5 ng/mL) stimulation. **(J)** Phagocytosis of pHrodo Deep Red E. coli BioParticles by macrophages in indicated treatments for 72h. Peripheral $CD14^+$ monocytes were treated with CMs of directly co-cultured monocytes with MSC(M), and mid- or late OA SF ± IL-6 neutralizing antibody (Ab, 2.5 µg/mL); 30% pooled mid- or late synovial fluid (SF). Gene expression in (F-H) and TNF soluble in (I) were assessed after 48h. Values are shown as mean ± SD; N=3 biological replicates; $n \geq 3$ technical replicates. An ordinary one-way ANOVA with Tukey's multiple comparisons test was used. Different letters indicate significant differences ($p < 0.05$) between groups; asterisks indicate significance ($p<0.05$) relative to untreated controls.

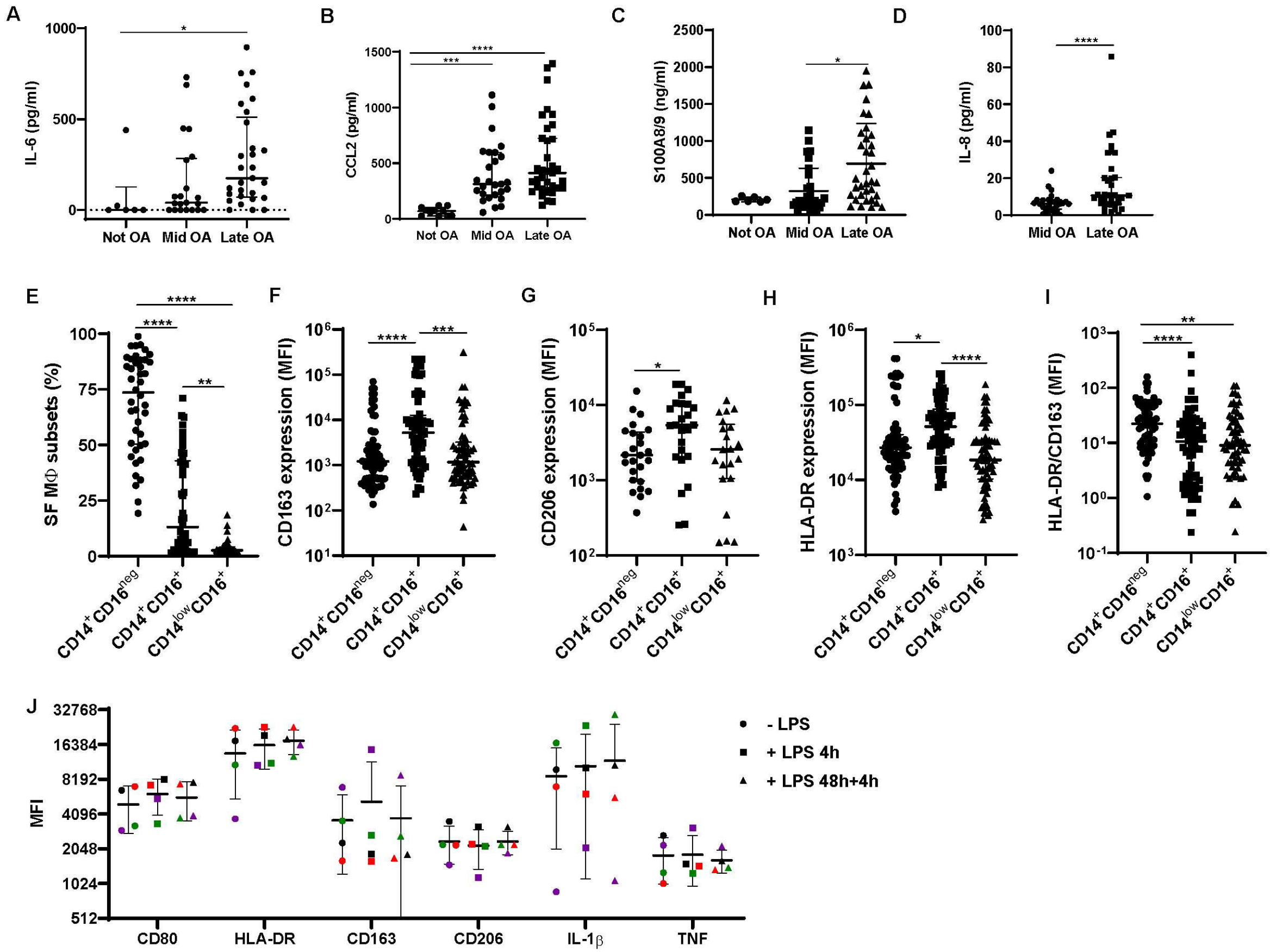
A
IL-6 (pg/ml)
Not OA
Mid OA
Late OA
B
CCL2 (pg/ml)
C
S100A8/9 (ng/ml)
D
IL-8 (pg/ml)
E
SF MΦ subsets (%)
F
CD163 expression (MFI)
G
CD206 expression (MFI)
H
HLA-DR expression (MFI)
I
HLA-DR/CD163 (MFI)
CD14+CD16neg
CD14+CD16+
CD14lowCD16+
J
MFI
CD80
HLA-DR
CD163
CD206
IL-1β
TNF
- LPS
+ LPS 4h
+ LPS 48h+4h

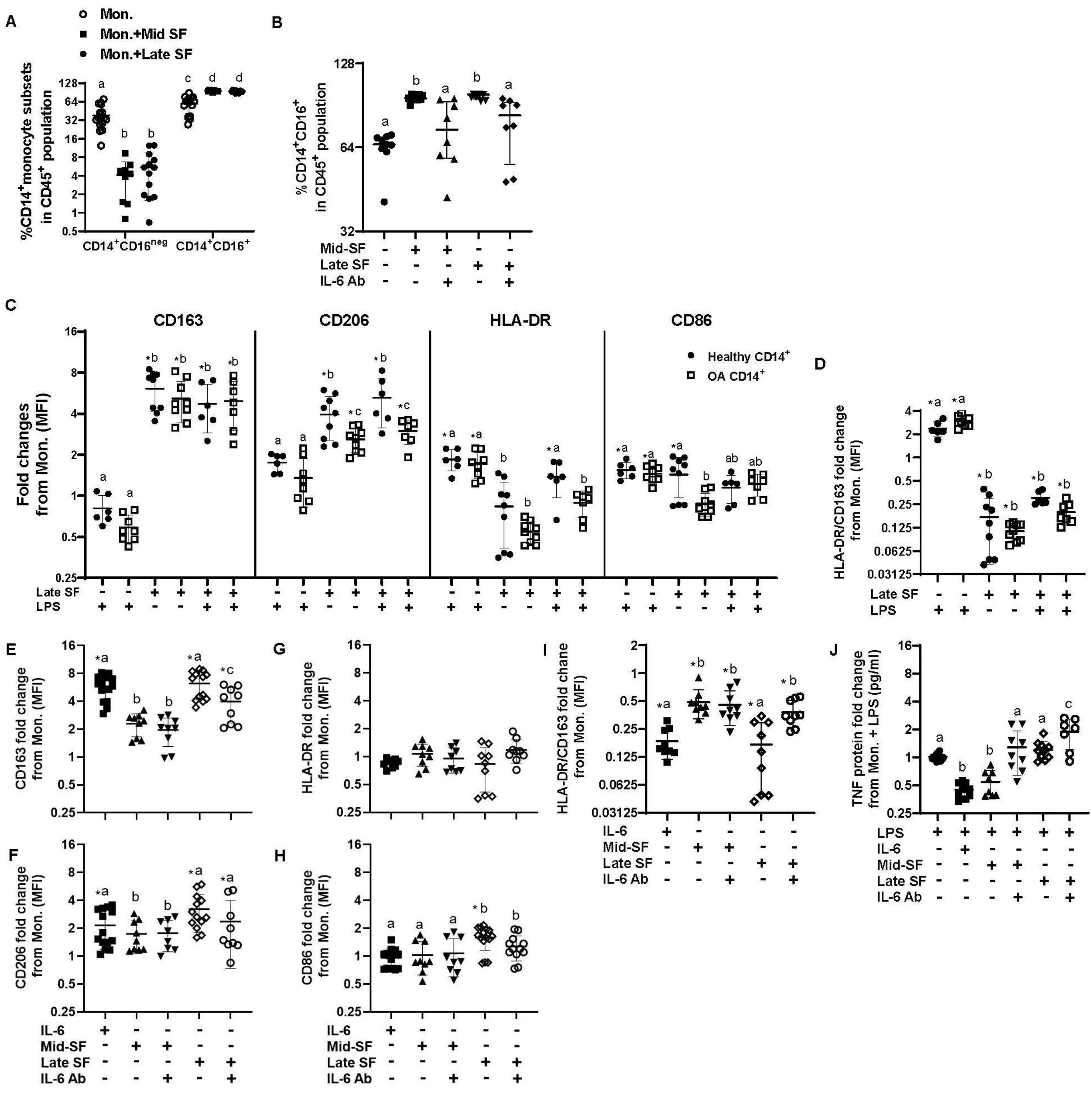
A
Mon.
Mon.+Mid SF
Mon.+Late SF
%CD14+monocyte subsets in CD45+ population
CD14+CD16neg
CD14+CD16+
B
%CD14+CD16+ in CD45+ population
Mid-SF
Late SF
IL-6 Ab
C
CD163
CD206
HLA-DR
CD86
Healthy CD14+
OA CD14+
Fold changes from Mon. (MFI)
Late SF
LPS
D
HLA-DR/CD163 fold change from Mon. (MFI)
E
CD163 fold change from Mon. (MFI)
G
HLA-DR fold change from Mon. (MFI)
I
HLA-DR/CD163 fold chane from Mon. (MFI)
IL-6
J
TNF protein fold change from Mon. + LPS (pg/ml)
F
CD206 fold change from Mon. (MFI)
H
CD86 fold change from Mon. (MFI)

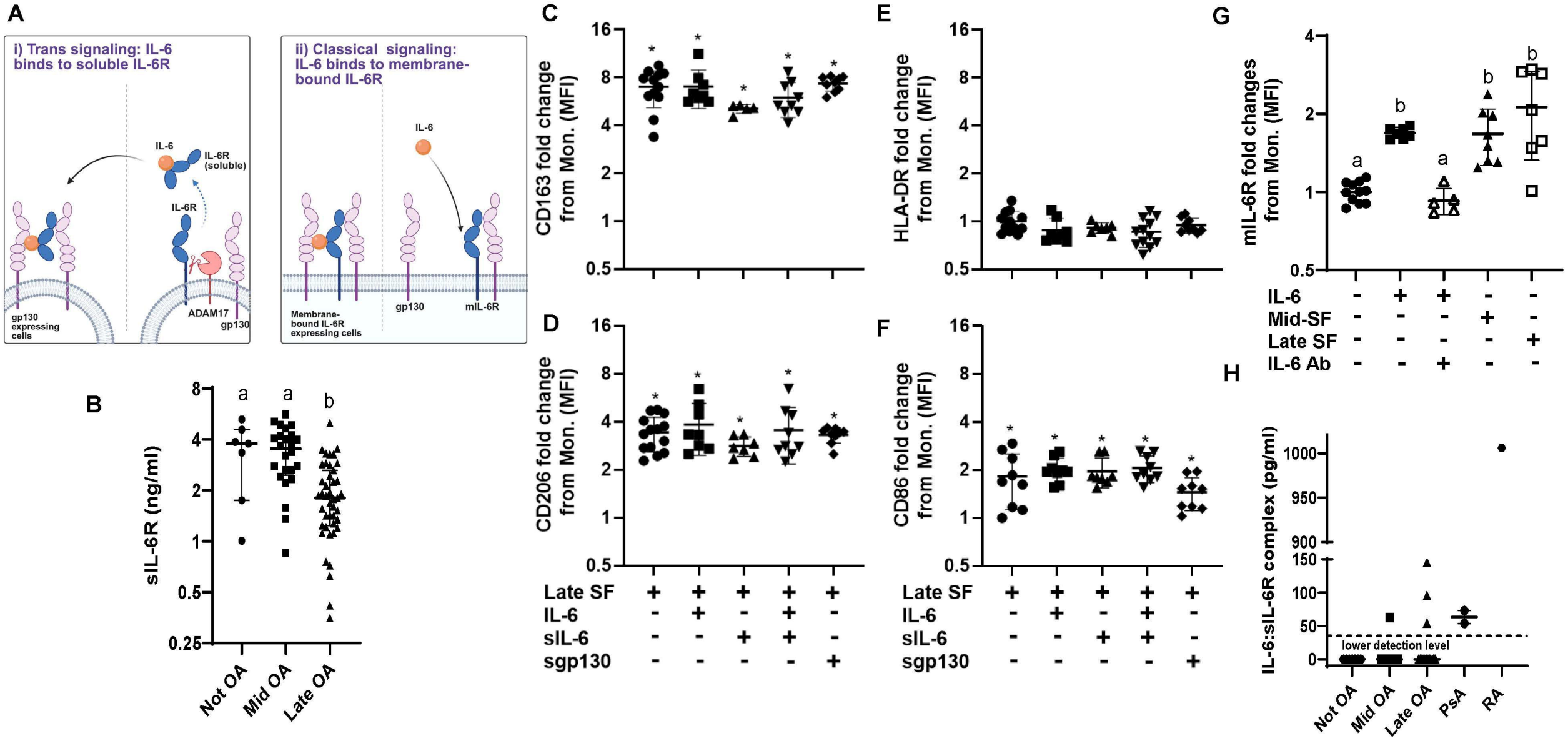
A
i) Trans signaling: IL-6 binds to soluble IL-6R
IL-6
IL-6R (soluble)
IL-6R
ADAM17
gp130
gp130 expressing cells
ii) Classical signaling: IL-6 binds to membrane-bound IL-6R
IL-6
gp130
mIL-6R
Membrane-bound IL-6R expressing cells
B
sIL-6R (ng/ml)
Not OA
Mid OA
Late OA
C
CD163 fold change from Mon. (MFI)
D
CD206 fold change from Mon. (MFI)
Late SF
IL-6
sIL-6
sgp130
E
HLA-DR fold change from Mon. (MFI)
F
CD86 fold change from Mon. (MFI)
G
mIL-6R fold changes from Mon. (MFI)
IL-6
Mid-SF
Late SF
IL-6 Ab
H
IL-6:sIL-6R complex (pg/ml)
lower detection level
Not OA
Mid OA
Late OA
PsA
RA

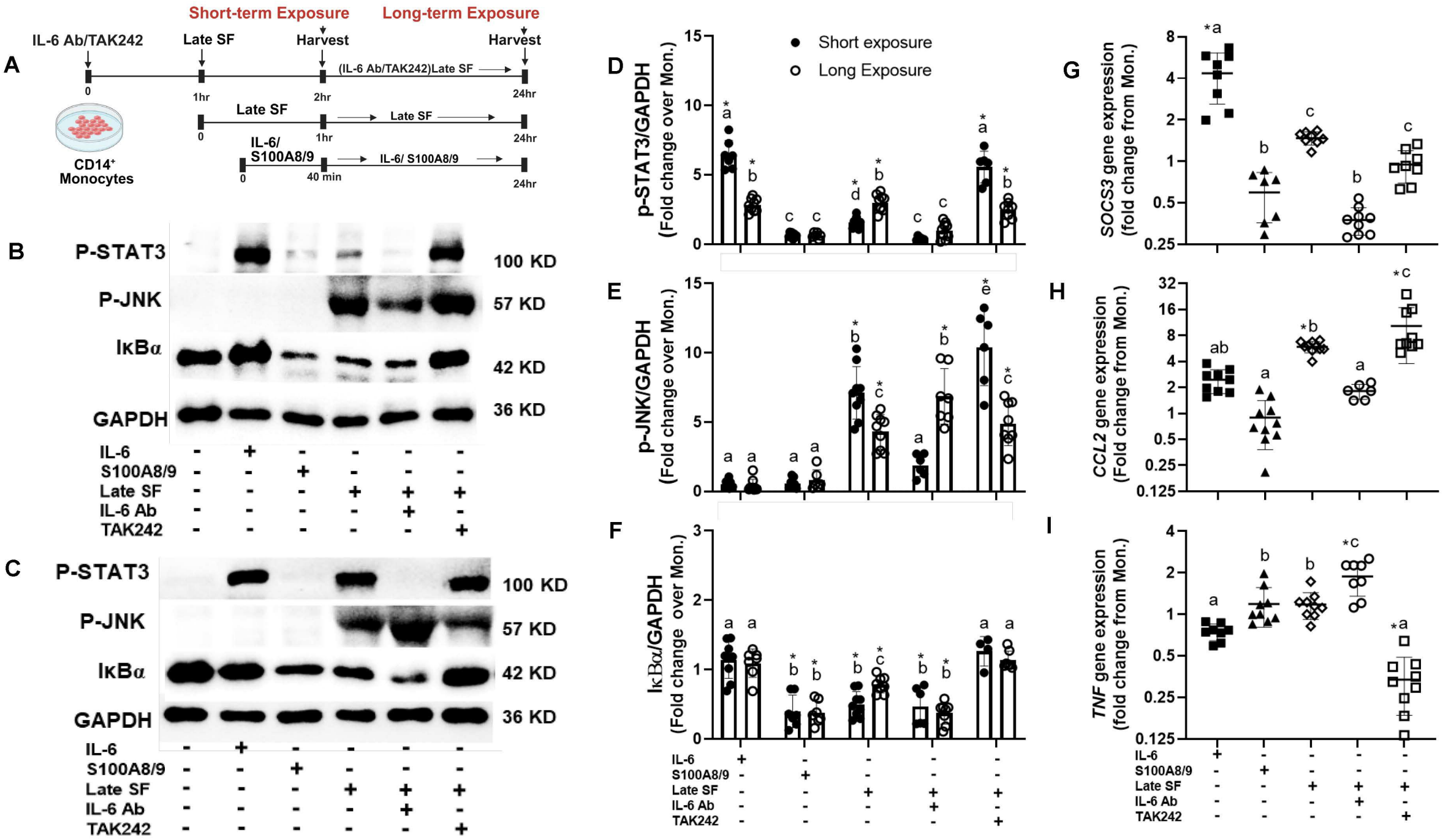
A
Short-term Exposure
Long-term Exposure
IL-6 Ab/TAK242
Late SF
Harvest
Harvest
(IL-6 Ab/TAK242)Late SF
0
1hr
2hr
24hr
Late SF
Late SF
0
1hr
24hr
IL-6/
S100A8/9
IL-6/ S100A8/9
0
40 min
24hr
CD14+
Monocytes
B
P-STAT3
P-JNK
IκBα
GAPDH
100 KD
57 KD
42 KD
36 KD
IL-6
S100A8/9
Late SF
IL-6 Ab
TAK242
C
P-STAT3
P-JNK
IκBα
GAPDH
100 KD
57 KD
42 KD
36 KD
IL-6
S100A8/9
Late SF
IL-6 Ab
TAK242
D
Short exposure
Long Exposure
p-STAT3/GAPDH
(Fold change over Mon.)
E
p-JNK/GAPDH
(Fold change over Mon.)
F
IκBα/GAPDH
(Fold change over Mon.)
IL-6
S100A8/9
Late SF
IL-6 Ab
TAK242
G
SOCS3 gene expression
(fold change from Mon.)
H
CCL2 gene expression
(Fold change from Mon.)
I
TNF gene expression
(fold change from Mon.)
IL-6
S100A8/9
Late SF
IL-6 Ab
TAK242

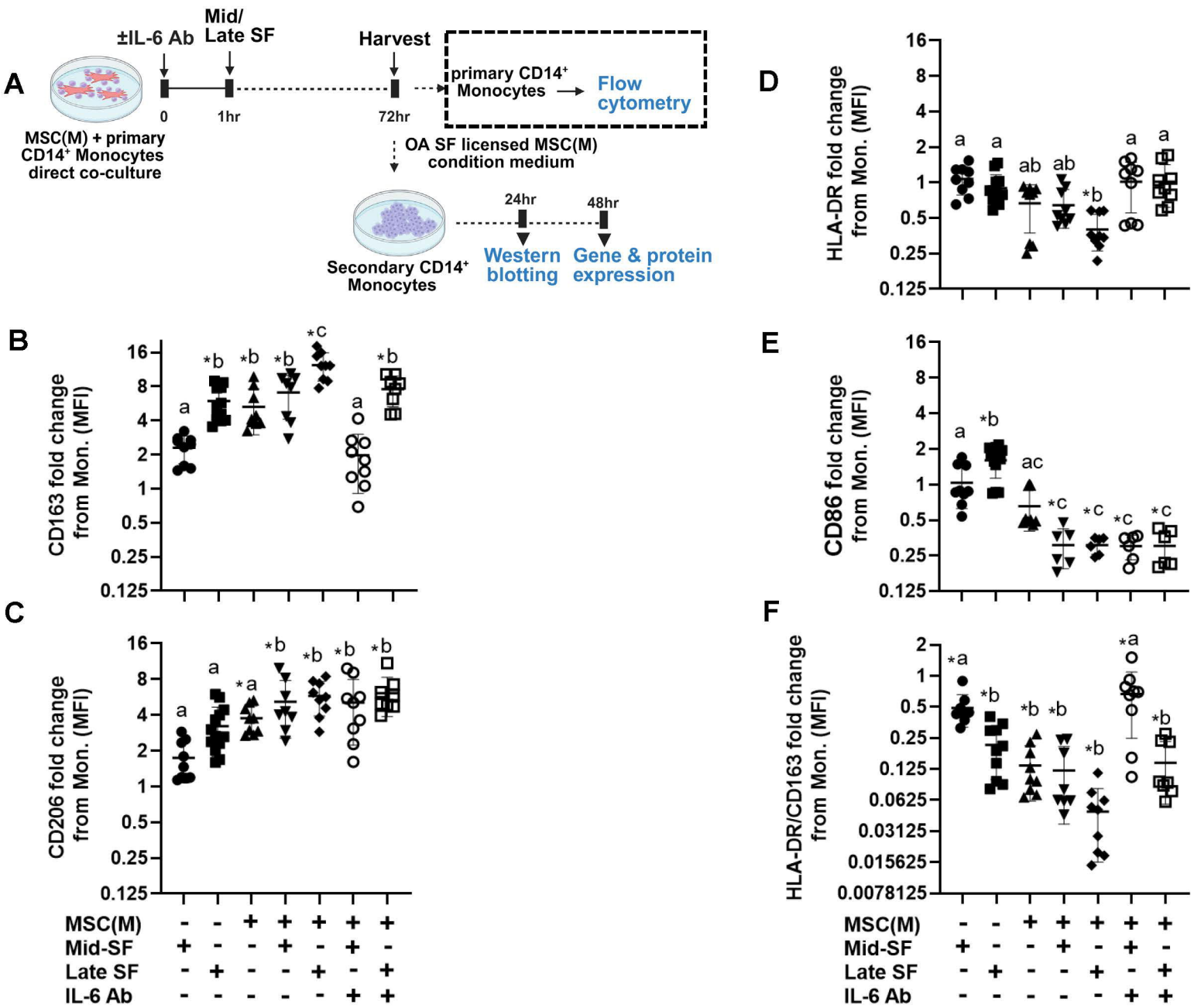
A
±IL-6 Ab
Mid/
Late SF
Harvest
0
1hr
72hr
MSC(M) + primary
CD14+ Monocytes
direct co-culture
primary CD14+
Monocytes
Flow
cytometry
OA SF licensed MSC(M)
condition medium
24hr
48hr
Secondary CD14+
Monocytes
Western
blotting
Gene & protein
expression
B
CD163 fold change
from Mon. (MFI)
C
CD206 fold change
from Mon. (MFI)
MSC(M)
Mid-SF
Late SF
IL-6 Ab
D
HLA-DR fold change
from Mon. (MFI)
E
CD86 fold change
from Mon. (MFI)
F
HLA-DR/CD163 fold change
from Mon. (MFI)

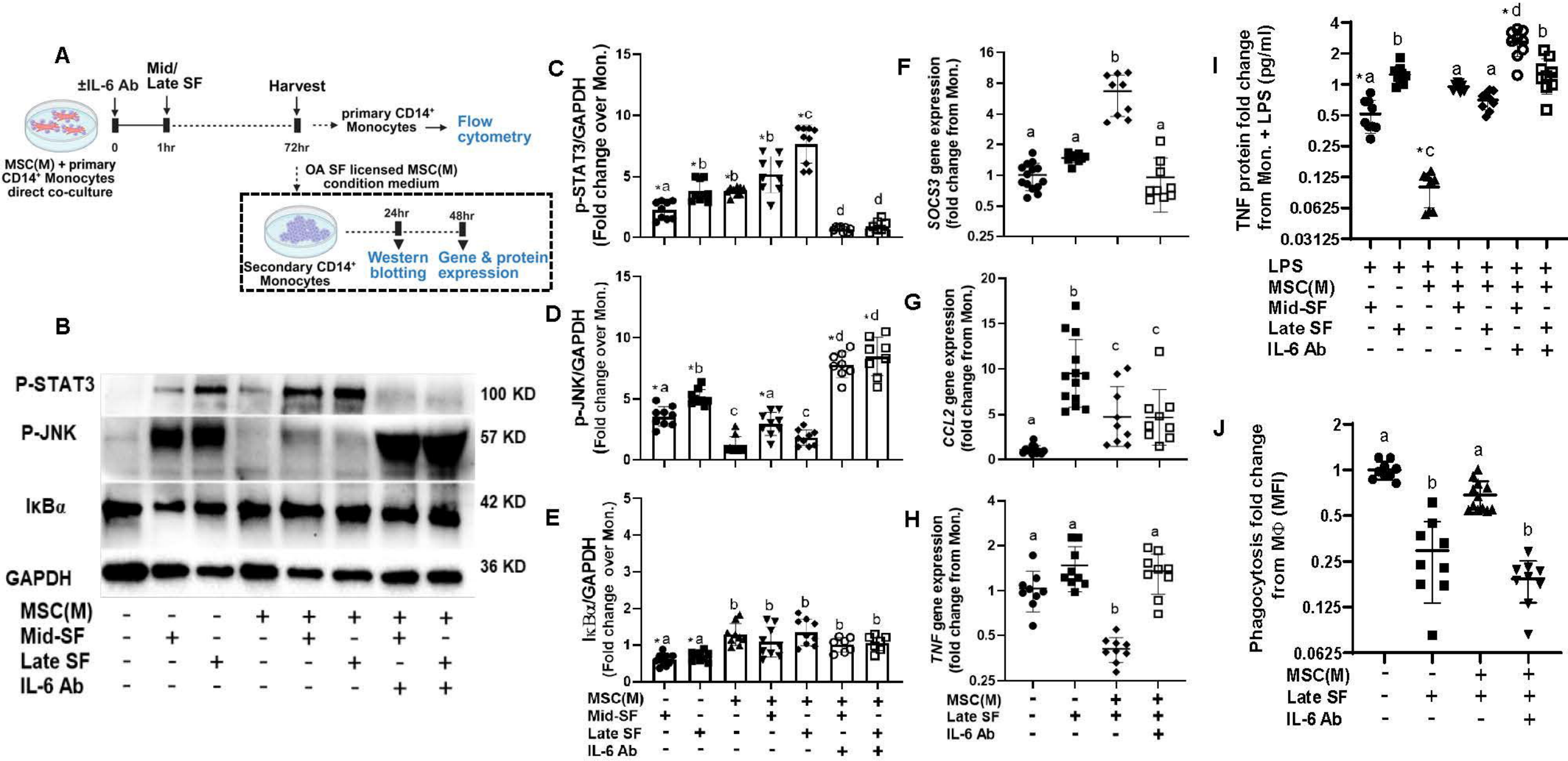
A
±IL-6 Ab
Mid/ Late SF
Harvest
0
1hr
72hr
primary CD14+ Monocytes
Flow cytometry
MSC(M) + primary CD14+ Monocytes direct co-culture
OA SF licensed MSC(M) condition medium
24hr
48hr
Secondary CD14+ Monocytes
Western blotting
Gene & protein expression
B
P-STAT3
P-JNK
IκBα
GAPDH
100 KD
57 KD
42 KD
36 KD
MSC(M)
Mid-SF
Late SF
IL-6 Ab
C
p-STAT3/GAPDH (Fold change over Mon.)
D
p-JNK/GAPDH (Fold change over Mon.)
E
IκBα/GAPDH (Fold change over Mon.)
F
SOCS3 gene expression (fold change from Mon.)
G
CCL2 gene expression (fold change from Mon.)
H
TNF gene expression (fold change from Mon.)
I
TNF protein fold change from Mon. + LPS (pg/ml)
LPS
J
Phagocytosis fold change from MΦ (MFI)